AD_____

AWARD NUMBER: DAMD17-01-1-0744

TITLE: Molecular Genetic Studies of Bone Mechanical Strain and of Pedigrees with Very High Bone Density

PRINCIPAL INVESTIGATOR: Subburaman Mohan, Ph.D.

CONTRACTING ORGANIZATION: Loma Linda Veterans Association for Research and Education
Redlands, CA 92374

REPORT DATE: November 2009

TYPE OF REPORT: Annual

PREPARED FOR: U.S. Army Medical Research and Materiel Command
Fort Detrick, Maryland 21702-5012

REPORT DOCUMENTATION PAGE

Form Approved
OMB No. 0704-0188

1. REPORT DATE	2. REPORT TYPE	3. DATES COVERED
1 November 2009	Annual	31 Oct 2008 – 30 Oct 2009

4. TITLE AND SUBTITLE

Molecular Genetic Studies of Bone Mechanical Strain and of Pedigrees with Very High Bone Density

5a. CONTRACT NUMBER

5b. GRANT NUMBER
DAMD17-01-1-0744

5c. PROGRAM ELEMENT NUMBER

6. AUTHOR(S)

Subburaman Mohan, Ph.D.

E-Mail: subburaman.mohan@va.gov

5d. PROJECT NUMBER

5e. TASK NUMBER

5f. WORK UNIT NUMBER

7. PERFORMING ORGANIZATION NAME(S) AND ADDRESS(ES)

Loma Linda Veterans Association for Research and Education
Redlands, CA 92374

8. PERFORMING ORGANIZATION REPORT NUMBER

9. SPONSORING / MONITORING AGENCY NAME(S) AND ADDRESS(ES)
U.S. Army Medical Research and Materiel Command
Fort Detrick, Maryland 21702-5012

10. SPONSOR/MONITOR'S ACRONYM(S)

11. SPONSOR/MONITOR'S REPORT NUMBER(S)

12. DISTRIBUTION / AVAILABILITY STATEMENT
Approved for Public Release; Distribution Unlimited

13. SUPPLEMENTARY NOTES

14. ABSTRACT
The primary goal of the proposed work is to identify the genes and their functions involved in mediating the anabolic response to mechanical stress. During the past year, we have used state-of-the-art technologies to investigate the role of a number of potential candidate genes in mediating skeletal anabolic response to mechanical loading. We found that modulation of leptin signaling influences mechanical loading response in the skeleton. We have also established using mice with conditional disruption of IGF-I in osteoblasts that local IGF-I expression in bone is essential for skeletal anabolic effects of exercise. On the other hand, disruption of formin- 2, a mechanoresponsive gene, did not influence skeletal anabolic response to mechanical loading. We believe that successful accomplishment of the proposed studies will provide a better understanding of the molecular mechanisms involved in identifying the genes and their function as related to mechanical stress.

15. SUBJECT TERMS
Mechanical strain, Quantitative trait loci analysis, microarray analysis, osteoblasts Signaling pathways, bone formation

16. SECURITY CLASSIFICATION OF:			17. LIMITATION OF ABSTRACT	18. NUMBER OF PAGES	19a. NAME OF RESPONSIBLE PERSON
a. REPORT	b. ABSTRACT	c. THIS PAGE			19b. TELEPHONE NUMBER *(include area code)*
U	U	U	UU	51	USAMRMC

Table of Contents

Page

Molecular Genetic Studies of Bone Mechanical Strain

Osteoporosis is a disease that is characterized by low bone density and poor bone quality: bone becomes more fragile and the risk of fracture is greatly increased, especially in hip, spine and wrists. To date, the annual economic burden of osteoporosis is $20 billion and is expected to reach $62 billion by the year 2020 (1). These numbers exceed the cost of congestive heart failure, asthma and breast cancer combined. Thus, one of the major goals of our current research is to reduce the incidence of osteoporosis.

One approach to prevent osteoporosis is to increase new bone formation. At present, physical exercise has been used as one of the strategies to maintain bone mass and prevent bone loss in humans. Numerous studies using different loading models in human and animals have demonstrated that loading stimulates bone formation while unloading decreases bone formation (2-5). The mechanism through which mechanical loading increases bone formation is mechanical stimulation which activates signaling receptors which in turn activates a cascade of intra-cellular signaling pathways. This is turn activates several cellular processes leading to an increase in bone formation. To date, a series of cellular and molecular events, particularly the intra- and intercellular signaling pathways, and the molecular components that regulate these pathways by responding to mechanical stimulation, have been investigated using *in vitro* models (6-12). The data generated from in vitro models, although informative, is limited by the fact that most of the data were obtained from homogenous osteoblast cells in cell cultures. These models lack the vital communication between various types of cells, such as osteocytes, osteoblast and osteoprogenitors cells, which have been shown to respond to ML. Thus, the molecular components that respond to ML *in vivo* have not been fully understood. Once these components have been identified, it will be able to elucidate their role in regulating bone formation. This in turn, leads to a better understanding of the complex series of cellular and molecular events involved in bone formation, thus providing strategic pharmacological intervention to enhance or maximize the osteogenic effects of exercise. Our technical objectives for the past year are as follows:

Technical objectives

1) Continue to generate IGF-I Knock out and control mice and evaluate skeletal anabolic response to four-point bending.
2) Continue the ongoing studies on the role of the leptin receptor signaling pathway in mechanical strain response in osteoblasts.
3) Evaluation of the role of formin-2 in mediating the mechanical loading response on the skeleton.
4) Evaluate if 14104M gene is a mechanosensitive gene.
5) Evaluate the influence of mechanical strain on bone regeneration.
6) Continue in vitro phosphorylation studies to identify signaling proteins that are activated by mechanical strain in KO and control mice.
7) Continue data analysis and prepare manuscripts for submission to peer review journals for publication.
8) Prepare final progress report for submission to TATRC.

Technical objective 1: **Continue to generate IGF-I Knock out and control mice and evaluate skeletal anabolic response to four-point bending.**

During the past year, we crossed Cre- recombinase transgenic mice [Cre gene was driven by the procollagen, type IαII gene (Col1α2-Cre)] with loxp mice in which exon 4 of the IGF-I gene is flanked by the *lox*P gene to generate Cre+ loxp+/+ (homozygous conditional IGF-I KO), and Cre negative loxp (control) mice for our studies proposed in technical objective 1. At three weeks of age, tail snips were collected from mice and DNA was extracted using a PUREGENE DNA Purification Kit (Gentra Systems, Inc., Minneapolis, MN) according to the manufacturer's protocol. Polymerase chain reaction (PCR) was performed to identify the different genotypes (homozygous IGF-I KO, heterozygous IGF-I KO and control mice. We used Cre-recombinase primer (F- TTA GCA CCA CGG CAG CAG GAG GTT and R-CAG GCC AGA TCT CCT GTG CAG CAT) and loxp primer (Primer 1, AGT GAT AGG TCA CAA AGT TCC; Primer 2, AAA CCA CAC TGC TCG ACA TTG and Primer 3, CAC TAA GGA GTC TGT ATT TGG ACC) for the genotyping. The following optimized conditions were used to perform the PCR reaction: 95°C for 2 minutes; 35 cycles at 95°C for 40 sec, 57°C for 40 sec, 72°C for 40 sec; 70°C for 40 sec. The PCR products were run on a 1.5% agarose gel and the image was taken with a chemilmager 4400 (Alpha Innotech Corp., San Leandro, CA). **Figure 1** shows an example of how the different genotypes can be identified. After weaning, the mice were segregated according to the genotype and maintained on standard laboratory chow until they become old enough to perform mechanical loading - 10 weeks.

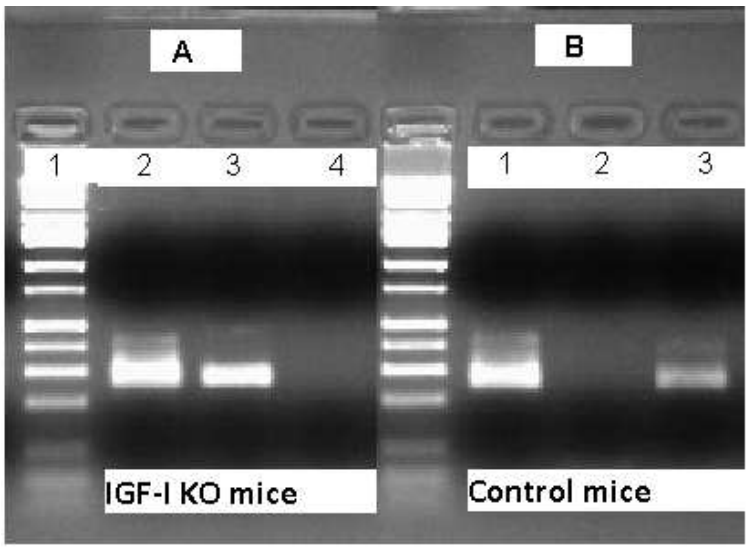

Image A: Row-1 marker, Row-2 GAPDH, Row-3 iCre, Row-4 IGF-I exon4

Image B: Row-1 marker, Row-2 GAPDH, Row-3 iCre, Row-4 IGF-I exon4

Figure 1: Genotyping of IGF-I KO vs. Control mice.

It is well established that the amount of mechanical strain exerted by a given load is largely dependent on the cross sectional area (moment of inertia) such that a mouse with a large cross sectional area will experience lower mechanical strain and vice versa for a mouse

with small circumference. Since bones of IGF-I KO mice have a smaller circumference than the age- and sex-matched control mice, we calculated the amount of mechanical strain produced by varying loads using a mathematical approach (Stephen C. Cowin: Bone Mechanics Hand book, 2nd edition, 2001, chapter: Techniques from mechanics and imaging) on both IGF-I KO and control mice. Our goal is to apply loads that produced an equivalent amount of strain in the KO and control mice such that the difference in bone anabolic response induced by mechanical load is due to lack of osteoblast derived IGF-I and not due to difference in mechanical strain caused by varying bone size (periosteal circumference). As shown in **figure 2**, 6N load in IGF-I KO mouse produces mechanical strain equivalent to 9N load in the control mice. Based on this data, adjusted loads were applied on both sets of mice using a four-point bending device (4). The loading was performed under Isoflurane anesthesia at 2Hz frequency, 36 cycles, once per day for 12 days. The right tibia was used for loading and the left tibia as internal contralateral control. After 48 hours of the last loading, skeletal changes were measured in the loaded and non-externally loaded tibia of both sets of mice by in vivo pQCT (4). The mice were then euthanized and tibias were collected for further experiments.

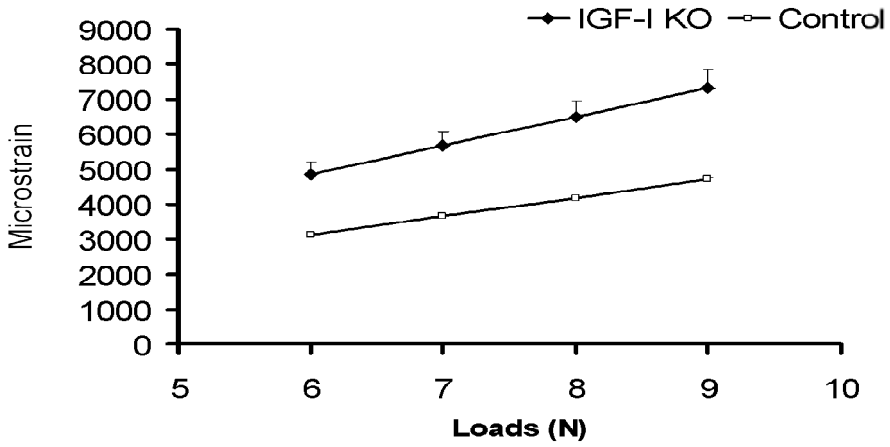

Figure 2: Mechanical strain generated for varying loads in the tibia of IGF-I KO and control mice. The y-axis corresponds to mechanical strain and x-axis corresponds to loads. N=5 mice. Values are mean ± SD.

Figure 3, shows that, in response to 12 days of four-point bending, the loaded bones of control mice showed significant increase in the newly formed bone while no such new bone formation was seen in the loaded bones of IGF-I KO mice **(Figure 3)**. Accordingly, skeletal parameters, such as total area, bone mineral content and bone mineral density, measured by pQCT, were significantly increased in the externally loaded bones when compared to non-externally loaded bones of control mice **(Figure 4)**. In contrast, in the IGF-I KO, many of these parameters showed little or no change in response to loading when compared to non-externally loaded bones of KO mice **(Figure 4)**.

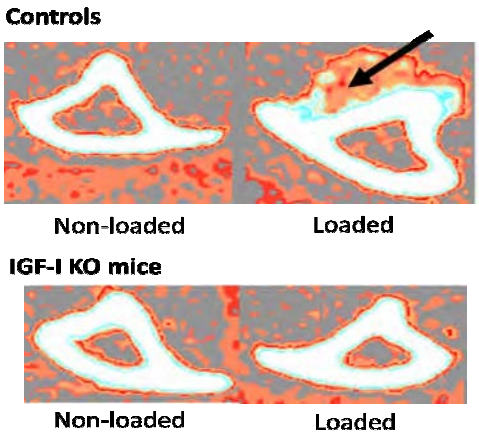

Figure 3: Cross sectional area of the externally loaded and non-externally loaded bones of IGF-I KO and control mice obtained from pQCT after 12 days of four-point bending. The arrow indicates the newly formed bone. The white color corresponds to cortical bone.

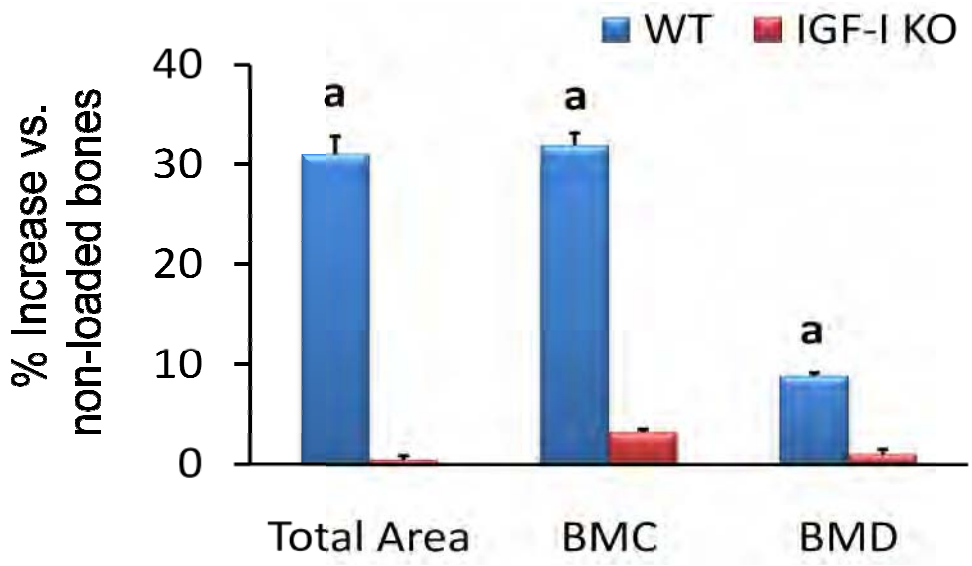

Figure 4: Changes in skeletal parameters measured by pQCT in response to 12 days of four-point bending in IGF-I KO and littermate control mice. The y-axis represents percent increase and x-axis represents bone parameters. Values are mean ± SEM. BMC, bone mineral content and BMD, bone mineral density. [a]$p<0.05$ vs. corresponding non-externally loaded tibiae, N=8/group.

It is known that application of load by the four-point bending technique produces pressure on the periosteal bone. Since there is a considerable amount of new bone formation on the periosteal surface of loaded bone, it is of concern whether the new bone formation response to loading by four-point bending is due to mechanical strain on the bone or due to

periosteal pressure. To rule out the possibility that the skeletal anabolic response induced by bending is not due to periosteal pressure, we performed a sham bending experiment in which the load was applied for the same period of time but not cyclically. In this study, we found that sham-loading neither increased periosteal bone formation nor caused changes in expression levels of bone marker genes, demonstrating that the skeletal changes induced by bending are not due to periosteal pressure (13). This finding also applies to the present study since we used the same loading model as well as regimen.

To further validate the pQCT measurements, we measured expression levels of bone marker genes and transcription factors induced by four-point bending in both control and IGF-I KO mice. The rationale for selecting these genes was based on previous studies (4, 14). We found that bone sialoprotein (BSP) and osteoblast specific factor 2 (OSF2) were increased by 2-2.5 fold in the loaded bones of IGF-I control mice while in the IGF-I KO mice, OSF2 decreased by 2.80 fold and no significant change was observed in BSP of the loaded bones **(Table-1)**. These findings, together, reveal that osteoblast derived IGF-I is critically important in mediating skeletal anabolic response to mechanical loading. Our findings also suggest that Runx2 is downstream of the IGF-I signaling pathway in the loaded bones. Additional studies are required to further validate the gene expression results.

Table 1: Quantitation of mRNA levels of bone genes in response to 12 days of four-point bending on 10 week female control and IGF-I KO mouse.

A) Control

Genes	**Non-Loaded**	**Loaded**	**P-value**	**Fold Change**
Bone sialoprotein	23.07 ± 0.14	21.77 ± 0.11	0.01	2.40 ± 0.17
Osteoblast specific factor 2	31.75 ± 0.22	30.37 ± 0.19	0.04	2.1 ± 0.09

B) IGF-I KO mice

Genes	**Non-Loaded**	**Loaded**	**P-value**	**Fold Change**
Bone sialoprotein	23.6 ± 0.15	23.99 ± 0.16	0.62	1.3 ± 0.2
Osteoblast specific factor 2	30.7 ± 0.2	32.3 ± 0.18	0.01	↓ 2.80 ± 0.2

N=5, the values mentioned above corresponds to Ct (cycles) obtained from real time PCR and are represented as mean ± SE.

One of the issues that is repeatedly raised against the four-point bending method of loading is that this model induces mainly periosteal bone formation since the mid diaphysis site at which loading is applied contains little or no trabecular bone. In terms of the pathogenesis of osteoporosis, it is known that loss of trabecular bone is a major contributor. Therefore, the next goal of our study was to select an in vivo loading model that can stimulate both trabecular and periosteal bone formation. To date, a number of loading models including jump exercise, wheel running and axial loading have been used to evaluate trabecular bone formation response. We chose the axial loading model because this model mimics exercise patterns of walking in humans and has been shown to induce both cortical as well as trabecular bone formation response to mechanical loading. Furthermore, studies have shown that axial loading on ulna or tibia results in robust increase in both cortical and trabecular bone formation after

two weeks of mechanical loading (15-20). Based on these rationales, we next evaluated the trabecular anabolic response to axial loading in both IGF-I KO and wild type mice.

To determine the effects of axial loading on bone formation response, we generated both male and female IGF-I KO mice and control mice as described above. Again, due to difference in bone size between KO and wild type mice, we measured mechanical strain produced by loads using strain-gauge technique at the metaphysis region of tibia. The strain data shows that female wild type and KO mice produced 825 με and 780 με, respectively. Similarly, the male wild type and KO mice produced 773 με and 745 με, respectively. Based on these data, adjusted loads were applied to both male and female IGF-I KO and wild type mice such that both sets of mice receive the same amount of mechanical strain. The loading was performed 40 cycles with 10 seconds rest between each cycle once per day for 3 alternative days for 2 weeks (15, 16).

In order to measure microarchitectural changes of trabecular bone and cortical bone changes in response to two weeks of axial loading we used Micro-CT, a high resolution tomography image system (Scanco In vivo CT40, Switzerland). Routine calibration was performed once a week using a three-point calibration phantom corresponding to the density from air to cortical bone. After the last day of loading, mice were euthanized and tibias were collected and stored in 1X PBS to prevent them from drying. Scanning was performed using 75Kv X-ray at resolution of 10.5 μm. To minimize the position error (slice positioning) and to be consistent in our sampling site from mouse to mouse, we undertook several precautionary steps, which include: 1) A scout view of the whole tibia was taken first in the micro-CT to determine landmarks and precise selections of measurement sites. 2) We used growth plate of the tibia as the reference point. 3) To measure trabecular parameters, we started our scan 30 slices away from the growth plate, which was 0.315 mm and progressing towards distal up to 0.840 mm providing a total of 50 slices (525 μm) and 3) Similarly, to measure cortical parameters, scanning was performed at 5.5 mm away from the growth plate and progressing towards distal up to 6.55 mm, providing a total of 100 slices (1050 μm). This area of scanning represents 37% positioning of the whole bone. After acquiring the radiographic data, images were reconstructed by using 2-D image software (as described by the manufacturer). The area of the trabecular bone was outlined within the trabecular compartment and a similar analysis was done for the cortical bone. Every 10 sections were outlined, and the intermediate sections were interpolated with the contouring algorithm to create a volume of interest, followed by three dimensional analysis using Scanco software. Parameters such as bone volume fraction (BV/TV, %), apparent density (mg HA/ccm), trabecular number (Tb.N, mm^{-1}), trabecular thickness (Tb.Th, μm) and trabecular space (Tb.Sp, μm) were evaluated in the loaded and non-externally loaded bones of both sets of mice. The values shown in Figure 5 are average of the above slices for each parameter. Since IGF-I KO mice are smaller in bone length compared to wild type littermate; we adjusted for this difference in length using standard calculation such that the sampling site is same for both sets of mice.

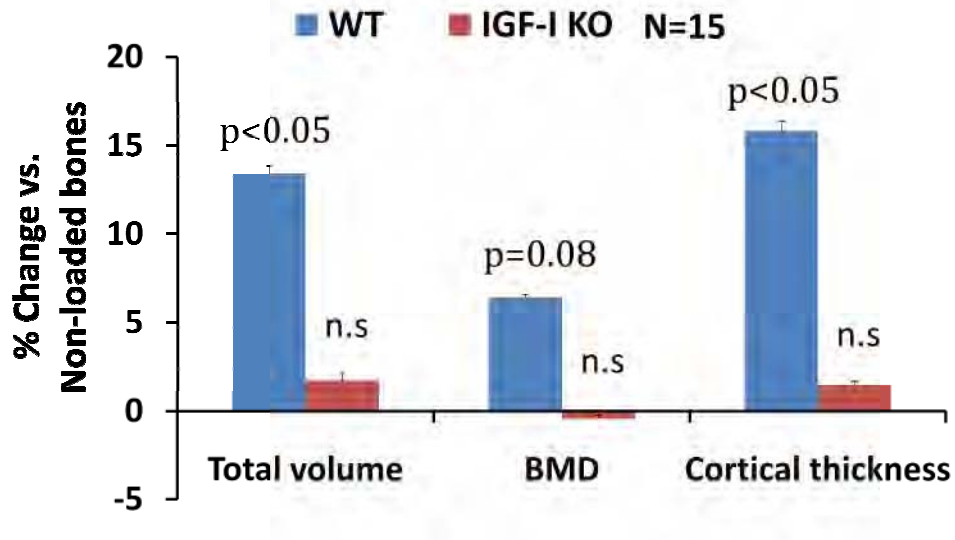

Figure 5: Changes in cortical parameters at the diaphysis measured by micro-CT at a resolution of 10.5 micron after 2 weeks of axial loading in IGF-I KO and wild type mice. The y-axis corresponds to % change and x-axis corresponds to bone parameters. The values are mentioned as Mean ± SE.

Consistent with the data we obtained from four-point bending, we found axial loading increased the amount of cortical bone in the wild type but not in the IGF-I knockout mice. Axial loading increased total volume, BMD and cortical thickness by 7 to 13% in the wild type,while in the IGF-I KO mice, little or no change was seen in these parameters in response to loading (**Figure 5**).

In addition to cortical bone, we measured loading induced changes in trabecular parameters. **Figure 6** shows micro-CT images of the loaded vs. non-loaded bones of both sets of mice. As you can see from Figure 6, the loaded tibia of control mice show a significant increase in the new bone compared to non-loaded tibia. While in the IGF-I KO mice, there is no difference between loaded and non-loaded tibia. Quantitative analysis shown in Figure 7 revealed that, in response to 2 weeks of axial loading, wild type mice show 18-20% increase in BV/TV, trabecular thickness and BMD with 5% increase in trabecular number. Thus, the mechanism through which axial loading increases trabecular bone in the wild type mice is largely by increasing the thickness of existing trabeculae rather than generating new trabeculae. This finding is consistent with previous published reports. Surprisingly, in the IGF-I KO mice, not only trabecular volume was not increased but we also observed a small decrease in the trabecular thickness in response to loading (**Figure 7**). Together, findings from both loading models demonstrates that loading increases cortical and trabecular bone response in the IGF-I control mice but not in the mice that are deficient in osteoblast-derived IGF-I.

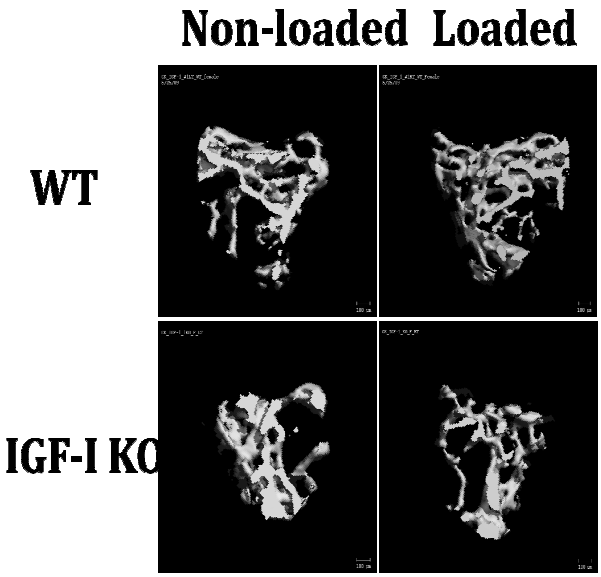

Figure 6: Micro-CT images of loaded vs. non-loaded trabecular bone of secondary spongiosa obtained from both wild type and IGF-I KO mice after 2 weeks of axial loading.

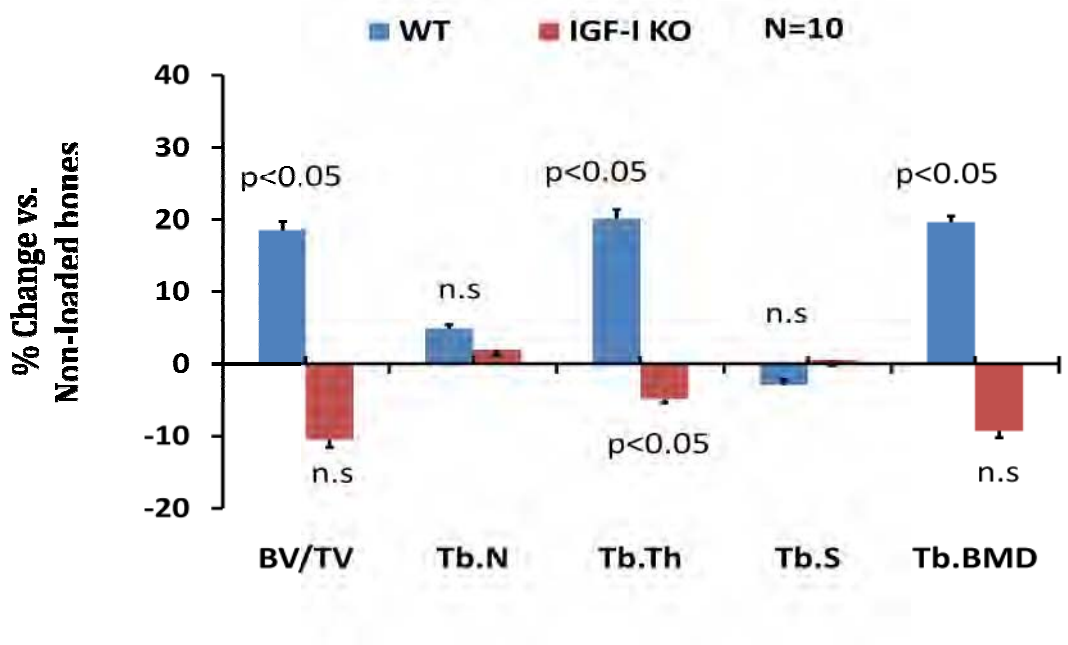

Figure 7: Micro-CT measurements of trabecular parameters of secondary spongiosa after 2 weeks of axial loading in the wild type and IGF-I KO mice. The y axis corresponds to percent change and x-axis corresponds to bone parameters. The values are mean ± SE, N=10.

In our data analyses, we combined data from both male and female mice of each group since in our past studies we did not find appreciable differences in skeletal anabolic response to mechanical loading between male and female mice. The increased cortical and trabecular bone volume in the loaded bones of control mice could be due to increased bone formation and/or decreased bone resorption. To evaluate the target cell types affected by mechanical loading, we are in the process of performing histology on the bones used for micro-CT analysis. In addition, we are also generating more IGF-I KO and wild type mice to perform gene expression studies to identify the signaling pathways impacted by the lack of IGF-I in the loaded bones. The outcome of this work will be reported in our next progress report.

Technical Objective 2: **Continue the ongoing studies on the role of leptin receptor signaling pathway in mechanical strain response in osteoblasts.**

In previous reports, we have presented compelling evidence that leptin receptor (Lepr) signaling pathway is a negative mechanosensitivity modulating gene or pathway. Briefly, heterozygous male and female leptin-deficient *ob*$^{-}$/*ob*$^{-}$ breeder mice (B6.v-Lep^{ob}/J) [in C57BL/6J genetic background] were obtained from the Jackson Laboratories (Bar Harbor, ME) to generate the *ob*/*ob* colony in our laboratory. The size (i.e., periosteal circumference, measured by pQCT) of tibia of *ob*$^{-}$/*ob*$^{-}$ mice was significantly bigger (by ~14%) than that of age-matched female C57BL/6J tibia (shown in previous report). Because the tibia of C57BL/6J mice with a smaller bone size had experienced a much higher strain at any given load than tibias of *ob*$^{-}$/*ob*$^{-}$ mice, a significant larger load is needed for C57BL/6J tibia than for *ob*$^{-}$/*ob*$^{-}$ mice to achieve an

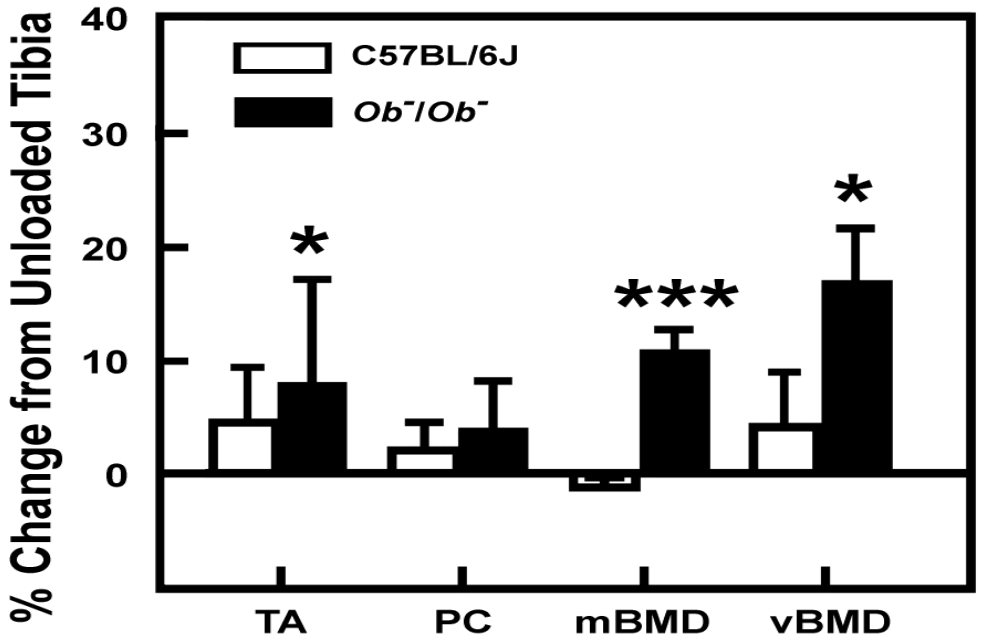

Figure 8: The bone responses in the tibia (by pQCT) of female *ob*$^{-}$/*ob*$^{-}$ mice (filled bars) after a 2-week 4-point bending exercise as opposed to those in the tibia of female C57BL/6J mice (open bars). The bending exercise was performed in six ob/ob mice and twelve C57BL/6J mice. The results are shown as relative percent change from the unloaded tibia of individual mouse (mean ± SEM). TA = total area; PC = periosteal circumference; mBMD = material bone mineral density; vBMD = volumetric BMD. *p<0.05; ***p<0.001.

equivalent mechanical strain (shown in previous report). By applying a similar mechanical strain to female *ob*$^{-}$/*ob*$^{-}$ mice (~2,100 με or a 9-N load) and to adult female age-matched C57BL6/J mice (~2,500 με or a 6-N load) in the form of 2-week four- point bending exercise, we found that this strain increased significantly total bone mineral content, cortical area, cortical content, cortical thickness, and material and volumetric bone mineral densities at the site of loading in *ob*$^{-}$/*ob*$^{-}$ mice but not in WT control mice (**Figure 8**), indicating that female *ob*$^{-}$/*ob*$^{-}$ mice exhibited an enhanced bone formation response to mechanical loading.

Our previous *in vivo* experiments utilized Leptin deficient rather than Leptin receptor (Lepr) deficient mice. In order to ensure that the observation seen with leptin-deficient mice was due to the lack of Lepr signaling and not indirectly through leptin deficiency, we sought to confirm that Lepr deficient mice also exhibited an enhanced osteogenic response to mechanical loading on periosteal bone formation in Lepr-deficient mice. For this work, we have established a Lepr KO mouse colony in our laboratory for investigation. Accordingly, we have purchased a breeding pair of heterozygous Lepr KO mice (B6.Cg-mLpr^{db}/+ +/J) from the Jackson Laboratories. Homozygous Lepr KO mice are infertile and cannot be used for breeding purposes. Because *Lepr*^{db} homozygotes are functionally sterile, the coat color marker misty (*m*) has been incorporated into stocks for maintenance of the diabetes (db) mutation. The misty mutation was introduced to produce repulsion double heterozygotes (*m* +/+ *Lepr*^{db}) for facilitating the identification of *Lepr*^{db} heterozygotes during breeding. Three types of littermates are produced from breeding these heterozygotes: the misty gray homozygote (m +/m +), the black *db* heterozygotes (*m* +/+ *Lepr*^{db}), and the black fat db homozygote (*Lepr*^{db}*+/ Lepr*^{db}*+*).

We have now obtained a colony of Lepr deficient mice. As was seen in leptin deficient mice, the size (periosteal perimeter) of tibia of 10-weeks-old female *Lepr*$^{-}$/*Lepr*$^{-}$ mice was also significantly smaller than that of tibia of age-matched female WT littermates (data not shown). Therefore, the load applied to the tibia has to be adjusted for each mouse strain, such that a similar mechanical strain is applied to the two mouse strains. Accordingly, a 9-N load was applied to the WT tibia, which yielded a strain of 4603 ± 256 μstrain; while a 7-N load was applied to the *Lepr*$^{-}$/*Lepr*$^{-}$ tibia, which produced a strain of 4549 ± 52 μstrain. The loading was applied at 2 Hz for 36 cycles, once a day for 12 days. The animals were then sacrificed one day after the last loading, and *de novo* bone formation at the loaded site and at the contralateral unloaded site of each animal was determined by pQCT.

Figure 9 shows that at the test mechanical strain (4,500-4,600 μstrain), the adult female WT littermates (in C57BL/6J genetic background) responded to the 12 days of daily mechanical loading with significant increases in total bone area, periosteal circumference, material bone mineral density, and volumetric bone mineral density by 5 to 10%. However, these bone responses of the age-matched female *Lepr*$^{-}$/*Lepr*$^{-}$ KO mice, which are in the range of 10-30%, were significantly much greater ($p<0.05$) than the bone responses in WT littermates. These results are consistent with the contention that Lepr and its signaling mechanism have negative regulatory actions on the mechanosensitivity of bone. These results also confirm that the enhancing effects of leptin deficient in *Ob*$^{-}$/*Ob*$^{-}$ mice were due to Lepr signaling and not other effects of leptin.

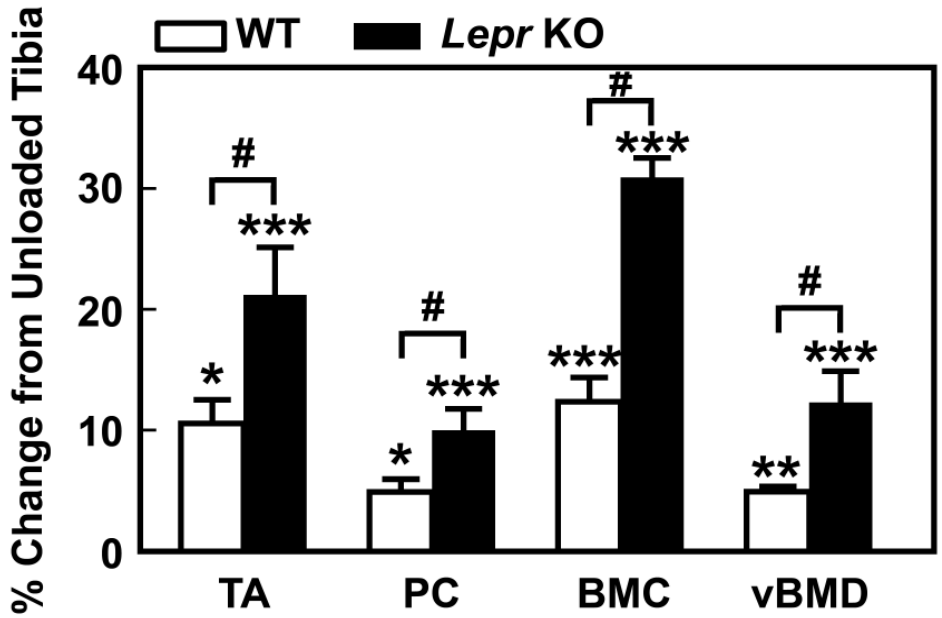

Figure 9: The bone responses in the tibia (by pQCT) of female *Lepr*$^{-}$/*Lepr*$^{-}$ mice (filled bars) after a 12 days of weekly 4-point bending exercise as opposed to those in the tibia of female WT littermates (open bars). The bending exercise was performed in six *Lepr*$^{-}$/*Lepr*$^{-}$ mice and six WT littermates. The results are shown as relative percent change from the unloaded tibia of individual mouse (mean±SEM). TA = total area; PC = periosteal circumference; mBMD = material bone mineral density; vBMD = volumetric BMD. *p<0.05; **p<0.01; ***p<0.001. #p<0.05 compared to WT littermates.

To further assess the role of the Leptin and/or the Lepr signaling on osteogenic response to mechanical stimulation, we next compared the biological responses of primary osteoblasts isolated from adult female WT C57BL/6J and from age-matched *ob*$^{-}$/*ob*$^{-}$ leptin deficient mice. We used a steady fluid shear stress as a surrogate of mechanical loading. In these studies, we have showed that the 30-min steady fluid shear of 20 dynes/cm^2 (which yielded mechanical stress to the cells that are within the physiological relevant range) produced significantly greater increases in [^{3}H] thymidine incorporation (an index of cell proliferation) in *ob*$^{-}$/*ob*$^{-}$ osteoblasts than those in C57BL/6J osteoblasts and osteoblasts of WT *ob*$^{+}$/*ob*$^{+}$ littermates (7).

These findings support the interpretation that deficiency in leptin and/or Lepr signaling led to an enhanced anabolic response to fluid shear stress in primary mouse osteoblasts. Moreover, we also showed that the enhanced mitogenic response to fluid shear in *ob*$^{-}$/*ob*$^{-}$ osteoblasts was completely obliterated by the leptin treatment (shown in previous report). These preliminary data together suggest that the *Lepr* signaling has a negative regulatory role in the context of mechanotransduction. These *in vitro* data are also consistent with the *in vivo* loading data that deficiency of leptin expression or *Lepr* signaling enhanced the osteogenic response to mechanical stimulation.

We next evaluated whether knocking down Lepr expression in C57BL/6J osteoblasts by specific siRNAs against leptin receptor would affect the fluid shear-induced Erk1/2

phosphorylation. For this work, a set of three small-interfering RNA duplex (siRNA) specific for mouse *Lepr* [i.e., *Lepr* siRNA1 (target sequence: CCC GAG CAA ATT AGA AAC AAA), *Lepr* siRNA2 (target sequence: ATC GAT GTC AAT ATC AAT ATA), and *Lepr* siRNA3 (target sequence: TTG AAG CTA AAT TTA ATT CAA)] and a non-silencing control siRNA without any homology to known mammalian genes were designed and synthesized by Qiagen. For the siRNA experiment, primary C57BL6/J (B6) or C3H/HeJ (C3H) mouse osteoblasts (a mouse strain that is relatively unresponsive to mechanical loading compared to the C57BL/6J mouse strain) were seeded at 60,000 cells in 24-well plate for 24 hr. The cells were tranfected with the test siRNAs using the HiPerFect Transcription reagent (Qiagen). Briefly, 3 µl of HiPerfect Transcription Reagent was added to 100 µl of DMEM containing 75 ng of *Lepr* or negative control siRNA duplex. The reaction mixture was incubated for 10 min at room temp and was then added to each cell culture well containing 500 µl of fresh DMEM and 10% FBS. After 16 hr of incubation at 37^{o}C, the medium was replaced by fresh DMEM containing FBS. The effectiveness of *Lepr* suppression was assessed by Western immunoblot using an anti-Lepr antibody after an additional 24-48 hrs of incubation at 37^{o}C. The protein loading was normalized against the cellular actin level using a specific anti-actin antibody. **Figure 10A** shows that the 24-hr treatment with *Lepr* siRNA2 reduced cellular leptin receptor protein level in B6 osteoblasts by >70%. The siRNA-mediated knockdown of *Lepr* expression in C3H osteoblasts also led to restoration of their mitogenic responsiveness ([^{3}H] thymidine incorporation) to the shear stress (**Figure. 10B**). These data support our contention that Lepr or its signaling is a negative regulatory mechanism in the context of mechanotransduction.

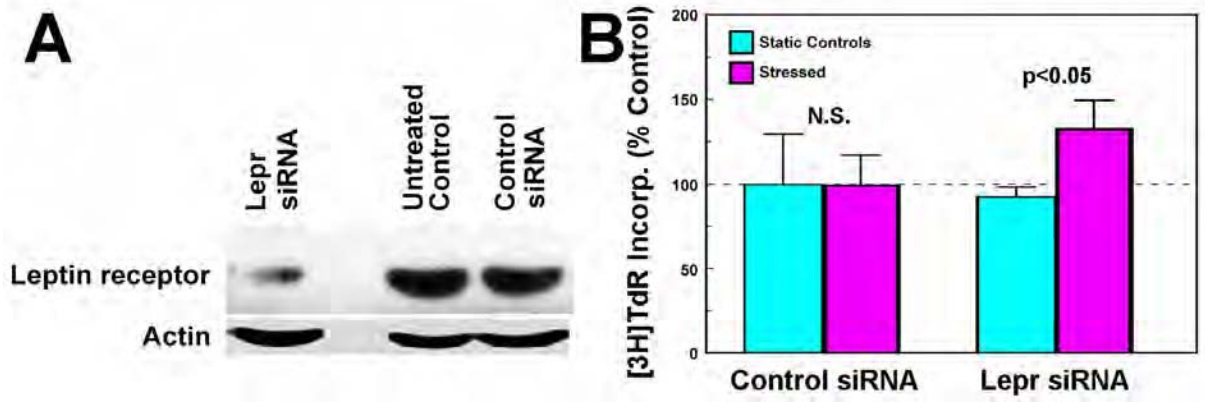

Figure 10: siRNA-mediated suppression of *Lepr* expression enhanced basal and shear [^{3}H] thymidine incorporation in C57BL/6J osteoblasts and restored the mitogenic response of C3H/HeJ osteoblasts to fluid shear *in vitro*. A shows the effects of the 24-hr treatment of a set of *Lepr* siRNAs (1-3) alone or in combination (at a total concentration of 5 nM) on the cellular *Lepr* protein level in C57BL/6J osteoblasts. Cellular *Lepr* protein was identified by Western blots and normalized against actin. B shows that suppression of *Lepr* expression in C3H/HeJ osteoblasts by a 24-hr treatment with 5 nM *Lepr* siRNA2 restored their mitogenic response to the 30-min fluid shear stress of 20 dynes/cm^{2}. Cell proliferation was measured by [^{3}H] thymidine incorporation during the final 6 hrs of a 24-hr incubation. Results are shown as mean ± SEM (n=4).

Technical Objective 3: **Evaluation of the role of formin-2 (FMN2) in mediating mechanical loading response on the skeleton.**

It is well known that exercise increases bone formation but the molecular components responsible for increased bone formation resulting from exercise are not well known. Identifying these molecules and their pathways may lead to a better understanding of how exercise maintains bone health and could lead to the development of a novel therapeutic strategy. To date, a number of signaling pathways activated by mechanical strain have been investigated using *in vitro* cell culture models. While the data generated from these models have identified new signaling pathways that are activated by mechanical strain, there are certain deficiencies with these models. For example, many of the in vitro models utilize homogeneous population of cells and lack vital communication between various types of cells and cell-matrix interactions that occur in vivo at the three dimensional level. Since little is known on the molecular components that are activated in the skeletal tissue in response to mechanical loading *in vivo*, we performed a genome wide microarray analysis using RNA extracted from a good responder C57BL/6J (B6) mouse to identify the mechanoresponsive genes. Of the 346 genes that were differentially expressed in the loaded bones compared to externally non-loaded control bones, we found formin-2 mRNA levels were increased significantly (21). Furthermore, we also found this gene to reside within the region of mechanical loading QTL, one of the major QTL (Chr 1, 96cM) that we identified in our study for bone response to mechanical loading **(Figure 11)** and by others for mechanical properties (13, 14). These findings let us to speculate that FMN2 may be involved in mediating the anabolic effects of ML on bone formation. Based on the above rationale and our preliminary data, we next tested the hypothesis that bone anabolic response is mediated by FMN2.

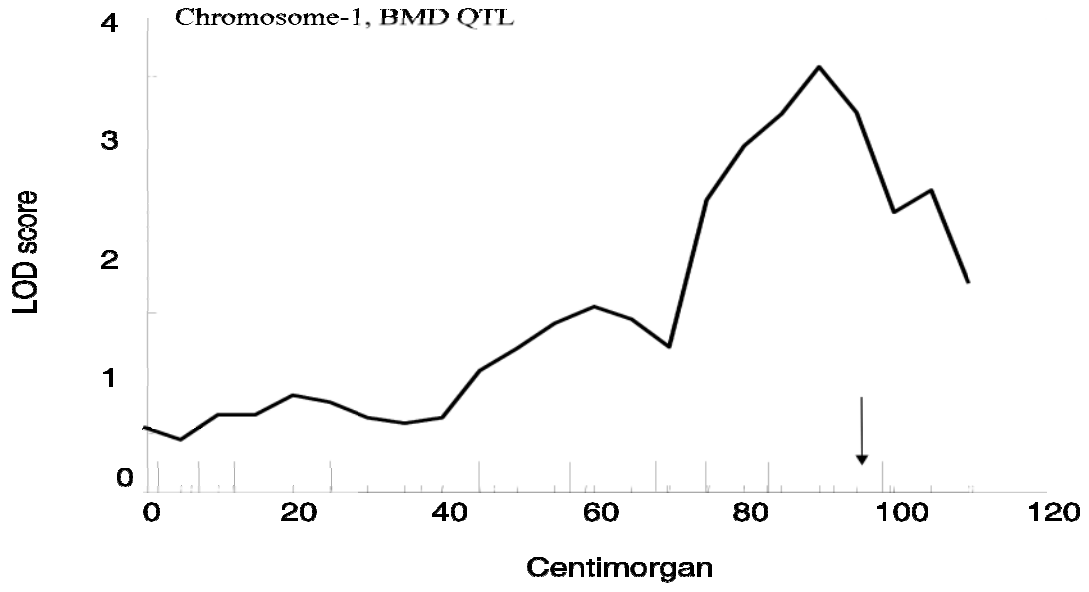

Figure 11: Detailed map of chromosome 1 showing significant BMD QTL. LOD scores between markers were determined using Pseudomarker MAINSCAN program with a default setting of 2.5cM between steps. The markers positions are highlighted as vertical lines in the x-axis. The y-axis corresponds to LOD score. The arrow indicates the location of gene FMN2 (96cM) on Chr 1.

To test the above hypothesis, we obtained FMN2 knockout mice from Dr. Philip Leder (Department of Human Genetics, Harvard Medical School, Howard Hughes Medical Institute, Boston, MA). These mice were originally generated in inbred 129Sv by homologous recombination of a targeting vector with 1300 bp of the FH1 domain of FMN2 deleted and replaced by 1257 bp containing the PGK-Neo gene followed by stop codons in all three reading frames. Two heterozygote FMN2 (+/-) male/female pairs were bred to generate wild type (+/+), and knock out (-/-) pups to perform the above study.

Before proceeding into the loading experiment, we measured bone size (periosteal circumference) of both KO and wild type mice by using pQCT. This is because the amount of mechanical strain exerted by a given load is largely dependent on the bone size (moment of inertia) such that a mouse with a larger circumference will experience lower mechanical strain and vice versa for a mouse with a small circumference. In order to assure that the difference in skeletal anabolic response to loading is due to lack of FMN2 gene and not due to difference in bone size, we measured bone size by pQCT in both control and FMN2 KO mice before initiation of loading experiment. We found that there was no difference in the bone sizes between the two sets of mice and therefore we chose to apply same mechanical load for both FMN2 KO and control mice. At 10 weeks, mechanical loading was performed using four-point bending device. A 9N load was applied on both control and FMN2 KO mice. The loading was performed at 2Hz Frequency, for 36 cycles, once per day. The loading was carried out for 2 weeks (6 day/week, 1 day rest) under Isoflurane anesthesia. The left tibia was used for loading and the right tibia was used as the contralateral control. After 48 hours of the last loading, mice were anesthetized with Isoflurane and skeletal changes were measured by pQCT in the loaded and non-externally loaded bones of both sets of mice. The results from our study show that skeletal parameters were increased significantly in the loaded bones compared to unloaded bones in both formin-2 KO and control mice, but no differences were observed between the two genotypes **(Figure 12)**. The lack of difference in the anabolic response to mechanical loading between the FMN2 KO and control mice was surprising and could be due to compensation by other members of the formin family in the knockout mice.

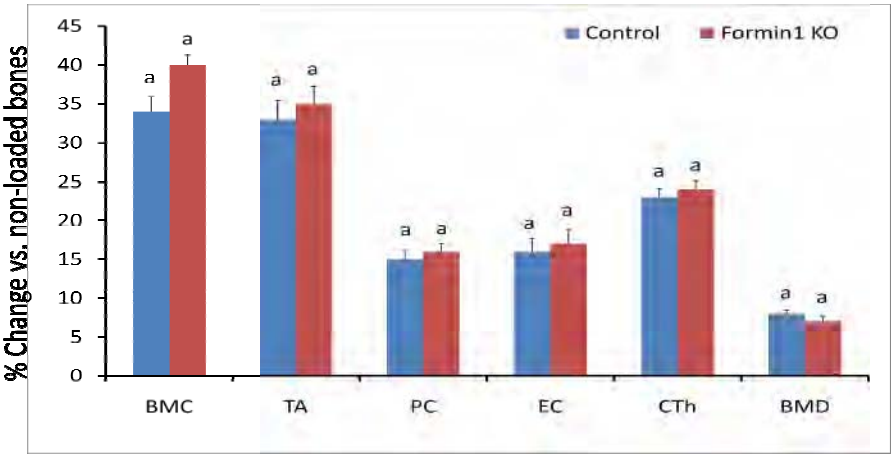

Figure 12: Changes in bone parameters measured by pQCT in response to 12 days of four-point bending on 10-week control and formin-2 KO mouse. The y-axis corresponds to percent change and x-axis corresponds to bone parameters. BMC; bone mineral content, TA; total area, PC; periosteal circumference, EC; Endosteal circumference, CTh; cortical thickness and BMD; bone mineral density. Values are mean ± SE, $^{a}p<0.05$ vs. non-externally loaded bones and N=7.

Technical Objective 4: **Evaluate if 14104M gene is a mechanosensitive gene**.

As a part of another army funded study, we used ENU (N-ethyl-N-nitrosourea) mutagenesis in the mouse model to identify genes that regulate bone density and bone size, two important determinants of bone strength. ENU is a powerful mutagen that causes base transverse and point mutation in the genome with which one can identify and study a phenotype of interest (22). Using this approach, our group established several lines of mutant mice that exhibit differences in bone size or bone density (23, 24). One such a mutant line, termed 14104M, exhibited large differences in bone size compared to corresponding control mice. Because we found large increases in periosteal bone formation in response to mechanical strain, we considered the possibility that 14104M gene is a mechanoresponsive gene. In order to identify the candidate gene responsible for the 14104 mutant phenotype, we have used 2 approaches; single nucleotide polymorphism (SNP) analyses and gene expression changes. These 2 strategies have been successfully used by us as well as others in the identification of QTL gene for a variety of complex phenotypes including bone density (25-29). The SNPs can change the encoded amino acids (nonsynonymous) or can be silent (synonymous) or simply occur in the noncoding regions. They may influence promoter activity (gene expression), messenger RNA (mRNA) conformation (stability), and subcellular localization of mRNAs and/or proteins and and thereby influence gene function. To identify the mutant gene, we are using a functional positional candidate gene approach in which candidate genes are identified within the mutant locus based on their known functions for subsequent sequencing the coding regions of selected candidate genes. **Table 2** represents the candidate genes selected for sequence analyses. For gene expression profiling, we have used microarray techniques to compare gene expression between RNA isolated from the mutant's bones and the wild type B6 bones. Identification of differentially expressed genes that are located within the mutant locus or signaling pathway affected in the mutant mice will lead to the identification of candidate genes.

Sequencing candidate genes

(1) Designed oligos to amplify the appropriate regulatory regions.

Using NCBI database, we have designed primers that over-lap with each other in order to cover the whole coding region of each gene; the primers used are described in **Table 3.**

(2) Prepare cDNA and PCR amplify the cDNA fragments from the mutant and B6 mice.

RNA was isolated from tissues obtained from B6 and 14104 mutant mice. cDNA was generated using M-MLV reverse transcription enzyme (Promega, Madison, WI, USA) . Then, after optimizing the PCR condition for every pair of primers, we prepared 5 x 100 µl PCR product from every segment and every strain (we used B6 and mutant DNA). Then the PCR products were purified using QIAquik PCR purification kit from Qiagen.

(3) Sequence the DNA fragments of regulatory regions. 5-20 ng from purified PCR products were sequenced using the ABI machine.

(4) Compare the sequence between congenic and B6 mice.

Table 4 represents a summary of the results of the sequencing. We have sequenced the coding regions of 5 candidate genes but no SNP was found between the 14104 mutant and the WT mice, only a small region at the 5'-end of the Cbx2 gene remains to be sequenced.

Expression profiling

For expression profiling, we have used cDNA chips from **Illumina** that carry 27 000 mouse genes and 37 000 probes, with 8 control genes spotted in 40-20 replicates. Among the 175 genes and EST in the region 109-119 Mb of chr 11, 10 showed significant difference ($P<0.05$) in the expression between the mutant (mut) and the wild type B6 (**Table. 5**). The genes that showed more than 1.9-fold change between the mutant and the wild type (WT) mice will be rechecked with real Time PCR. Then, the gene(s) differentially expressed between the mutant and the WT will be sequenced to identify the mutation that caused the difference in the expression.

Table 2: Selected candidate genes from the 14104 mutant locus.

Symbol, Name	**Known Molecular or Cellular Function related to bone**	**Skeletal Phenotype of Targeted Disruption**
Axin2, Axin 2	Negatively regulates expansion of osteoprogenitors and maturation of osteoblasts	Skeletal defects, craniosynostosis
Slc9a3r1, solute carrier family 9 (sodium/hydrogen exchanger), isoform 3 regulator 1	osteoblast differentiation	Hypophosphatemia and premature death
Sox9, SRY-box containing gene 9	Transcriptional regulation of osteoblast	Skeletal dysplasias
Grb2, growth factor receptor bound protein 2	Intracellular signaling cascade, Negative regulator of osteoclastogenesis and osteoblast differentiation	Enhanced Bone Volume, Craniofacial
Cbx2, chromobox homolog 2 (Drosophila Pc class)	chromatin assembly or disassembly	Mutations cause malformations of the axial skeletal
Socs3, Suppressor of cytokine signaling	Involved in GH signaling (JAK2)(STA5) in osteoblasts and regulates CD11c+ dendritic cell-derived osteoclastogenesis	Decreased embryo size, increased resistance to induced-obeseity diet, weigh loss

Table 3: The sequences of the primers used for sequencing.

Symbol	Name	Sequence
Axin2	Axin2	5'-AGCCCCTGCTGACTTAAGAG
		5'-GTTCATCTGCCTGAACCCAT
		5'-TAGGCGGAATGAAGATGGAC
		5'-TGGGGAGGTAGCCACATAAG
		5'-GGCAGTGATGGAGGAAAATG
		5'-CACGTAGGTTCCGGCTATGT
		5'-AGAGGTGGTCGTCCAAAATG
		5'-AGAAAAGGAGGGGTCTGAGC
		5'-ACCTCTGCTGCCACAAAACT
		5'-CAAGACCAAGGAGGAGATCG
		5'-CAGGCTTCCTCTAGCTGTGC
		5'-AGCTACCCATTGGAGTCTGC
		5'-GCTGAGCTGCTCCTTGAAGT
		5'-AAGAGCCAAAGAAACTGGCA
		5'-GTCCCTCCCTAGGCTTTGTC
		5'-CTGCGATGCATCTCTCTCTG
Slc9a3r1	solute carrier family 9 (sodium/hydrogen exchanger), isoform 3 regulator 1	5'-GAGAAAGGTCGTGAGTCCCC
		5'-GCTTGTTCGGACTTCTCCTG
		5'-CGGTGAGAATGTGGAGAAGG
		5'-CCTTGTCTACCACCAGCAGC
		5'-TTGTGGAGGTCAATGGTGTC
		5'-AAGGGGAGCTAGGTAGGGTG
Sox9	SRY-box containing gene 9	5'-GGCAGCTGAGGGAAGAGGAG
		5'-TCCAGAGCTTGCCCAGAGTC
		5'-CAGGAAGCTGGCAGACCAGT
		5'-TGTTGGAGATGACGTCGCTG
		5'-TTGATCTGAAGCGAGAGGGG
		5'-TAGGAGATCTGTTGCGGGGA
		5'-CTGAGCCCCAGCCACTACAG
		5'-CTGGAATCCCAGCAATCGTT
Grb2	growth factor receptor bound protein 2	5'-CATTGTGTGTCCCAGTGTGC
		5'-CTTCACCACCCACAGGAAAT
		5'-GAGCCAAGGCAGAAGAAATG
		5'-AGTTGCAACCCAATGAGAGG
Cbx2	chromobox homolog 2 (Drosophila Pc class)	5'-CTTTGTGTGCAGCAGTGAGC

		5'-TTTTTCTGAGGCACTGGATG 5'-ATCCAAATCCAGCAGTTCGT 5'-AACCTGACTCTGGCTCATGC 5'-GCCAGTCTGATGAAAGGCAT 5'-TCAGCTTTTCCCCTTTGTTG 5'-GGCTATTCCTGCTACCAACC 5'-TCTCAGGACAGGGCAGAGTT
Socs3	Suppressor of cytokine signaling	5'-TAGACTTCACGGCTGCCAAC 5'-CCCTCACACTGGATGCGTAG 5'-GTTGAGCGTCAAGACCCAGT 5'-GGCTGGATTTTTGTGCTTGT

Table 4: Summary of the sequencing progress

Symbol, Name	Coding sequence (bp)	Region already sequenced (bp)	SNPs found (region remained to be sequenced bp)
Axin2, Axin 2	350-2872	230-3024	none
Slc9a3r1, solute carrier family 9 (sodium/hydrogen exchanger), isoform 3 regulator 1	186-1253	126-1315	none
Sox9, SRY-box containing gene 9	353-1876	273-2064	none
Grb2, growth factor receptor bound protein 2	332-985	210-1128	none
Cbx2, chromobox homolog 2 (Drosophila Pc class)	81-1640	423-1726	None (81-422 bp)
Socs3, Suppressor of cytokine signaling	377-1054	264-1136	none

Table 5: Genes at 109-119 Mb in chr 11 that showed significant difference between the 14104 mutant and the wild type B6 mice.

Symbol, Name	Description	ttest (P value)	Fold-change1*	Fold-change2#
2600014M03Rik	EST	0.007815	2.22757103	1.326567
Slc39a11	Solute carrier family 39 (metal ion transporter), member 11	0.008198	0.811734	1.36306375
2310075G12Rik	EST	0.013453	0.814241	1.36727384

Rhbdl6	Rhomboid 5 homolog 2 (Drosophila)	0.019647	1.349861	2.26668677
Sdk2	Sidekick homolog 2 (chicken)	0.026345	1.222787	2.05330424
Kctd2	Potassium channel tetramerisation domain containing 2	0.026628	0.861888	1.44728288
1700012B07Rik	EST	0.031338	1.262735	2.12038517
Recql5	RecQ protein-like 5	0.041487	1.157285	1.94331246
BC034097	EST	0.045313	1.302127	2.18653082
Evpl	Envoplakin	0.046496	1.23859	2.07984009

*Fold-change before normalization and # after normalization with all control genes in the chip

To determine whether the genomic region responsible for the 14104M phenotype is also responsible for mediating or regulating anabolic effects of mechanical loading on bone formation, we propose to evaluate the bone anabolic response to mechanical loading in 14104 mutant and corresponding control mice.

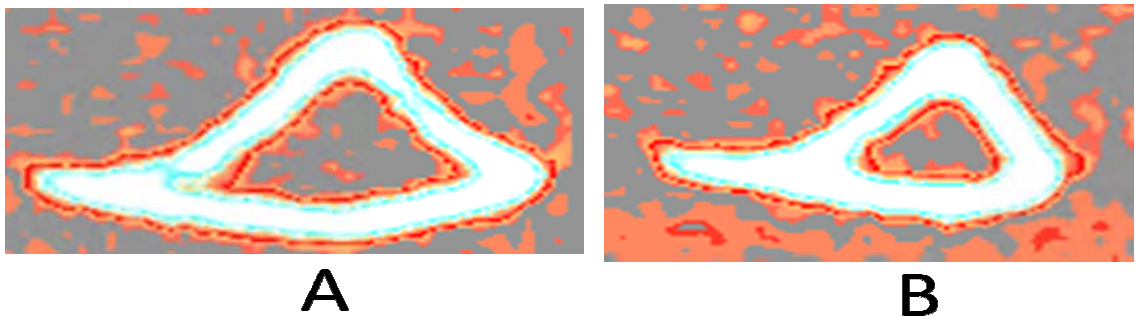

Figure 13: Cross sectional area of the right tibia obtained by pQCT in female A) littermate control mice and B) 14104 mutant mice.

To obtain mutant and control mice for mechanical loading studies we have crossed 14104 female mutant mice with C57BL/6J male mutant mice to generate pups. At 9 weeks, we performed in vivo pQCT on the tibia of these mice to screen for mutant and littermate control. We choose periosteal circumference as an endpoint to differentiate the mouse lines. Quantitative analysis revealed a group of mice with reduced periosteal circumference (4.42 mm) compared to another group of mice whose periosteal circumference (5.01 mm) was very similar to the control C57BL/6Jmice. **Figure 13** shows cross sectional area of the female mutant mice versus littermate control mice. Based on this phenotypic difference, we segregated the

mice into two groups: mutant and wild type. Once these mice reach 10 weeks they will be subjected to mechanical loading to evaluate the skeletal anabolic response. The rationale for selecting 10 week age for the mechanical loading study is based on our findings from our previous age-related study.

Before proceeding into the loading experiment, we next measured mechanical strain on the tibia of both mutant and wild type mice. This is because, the mechanical strain generated by a given load depends largely on bone size, and therefore, we predict that mice with smaller circumference tend to produce more mechanical strain than mice with larger circumference. In order to assure that the difference in bone anabolic response to mechanical loading between 14104 mutant and wild type mice is not due to difference in mechanical strain produced due to bone size differences, we measured mechanical strain by using strain gauge technique on tibia of 10 week ENU mutant mice and wild type mice. The results from our study shows that female mutant mice produced 600 με (N=4) and wild type female mice produced 370με (N=4) for a 6N load. Based on these data, we propose to apply 6N load to female mutant mice and 10N load to female wild type mice such that both mice receive same amount of mechanical strain. Currently, we are in progress of measuring the strain rate for loads on male mice. We are also crossing 14104M female mutant with 14104 male mutant mice to generate more pups. We intent to use some of these pups for strain gauge experiment since we need more data points to validate above strain data and the rest will be used for axial loading once the appropriate load is selected which is based on the strain-gauge data.

Technical Objective 5: Evaluate the influence of mechanical strain on bone regeneration. These studies will be undertaken during the remainder of the no-cost extension period (i.e. Nov 09-Oct 10).

Technical Objective 6: **Continue in vitro phosphorylation studies to identify signaling proteins that are activated by mechanical strain in KO and control mice**.

Our previous studies have shown that mechanical transduction in osteoblasts involves protein-tyrosine phosphorylation of key signaling proteins, including Ekr1/2 (shown in previous report), that is known to mediate various anabolic signaling pathways (6,7). Accordingly, to further test if deficiency of leptin or *Lepr* signaling would lead to an enhanced osteogenic response to mechanical stimuli, we also examined the effects of a steady fluid shear on Erk1/2 phosphorylation in osteoblasts isolated from adult female *ob/ob* mice as opposed to those in adult female B6 osteoblasts *in vitro*. For comparison, osteoblasts of the WT littermates of *ob*/*ob* mice (ob^+/ob^+) were included. In addition, to evaluate whether the increase in Erk1/2 phosphorylation was associated with an osteogenic effects, we also measured [^{3}H]thymidine incorporation in this experiment. The data represented in **Figure 14** confirms that a 30-min steady fluid shear of 20 dynes/cm^2 significantly stimulated [^{3}H] thymidine incorporation and Erk1/2 phosphorylation in female B6 osteoblasts. The same shear stress produced significantly greater increases in [^{3}H]thymidine incorporation and Erk1/2 phosphorylation in ob^-/ob^- osteoblasts than those in B6 osteoblasts and osteoblasts of WT ob^+/ob^+ littermates. The shear stress-induced [^{3}H]thymidine incorporation and Erk1/2 phosphorylation in WT ob^+/ob^+ osteoblasts were not different from those in B6 osteoblasts. These results are highly

reproducible and were seen in every repeat experiment. **Figure 15** shows that down-regulation of *Lepr* expression in C57BL/6J osteoblasts by *Lepr* siRNA2 enhanced both basal (i.e., static control) and fluid shear-induced Erk1/2 phosphorylation much further in C57BL/6J osteoblasts, indicating that regulation of mechanosensitivity by leptin and/or Lepr signaling also involves mediation of protein-tyrosine phosphorylation of Erk1/2 in osteoblasts.

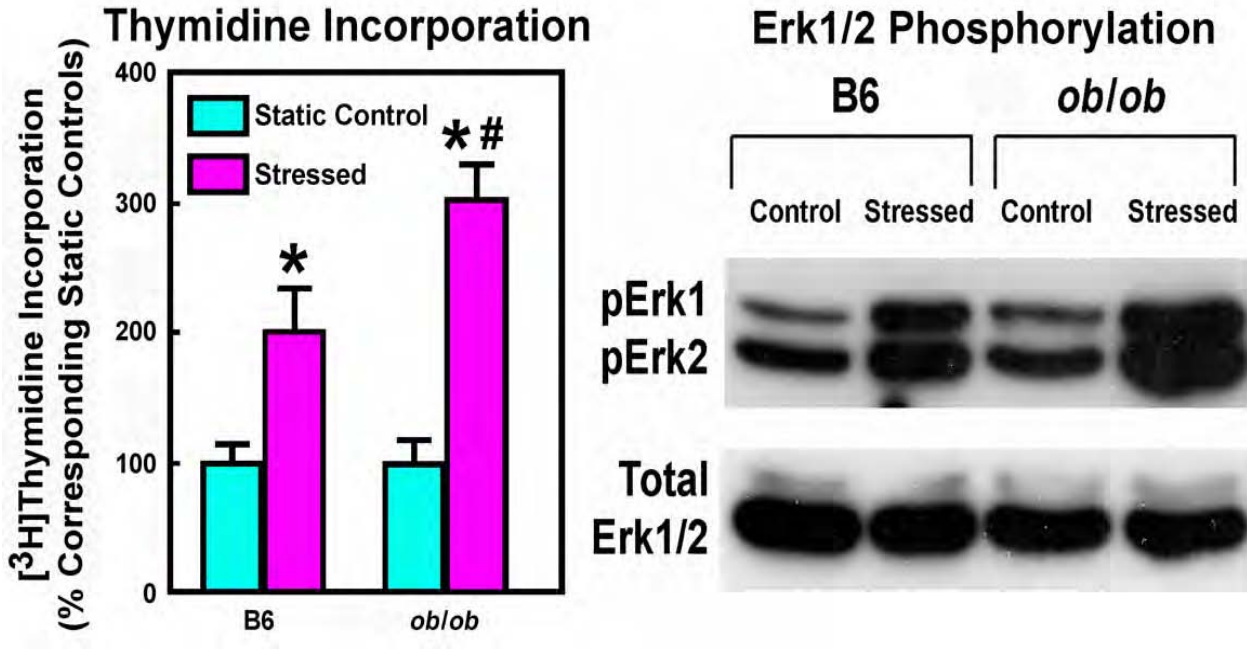

Figure 14: Effects of fluid shear on [^{3}H]thymidine incorporation (left) and Erk1/2 phosphorylation (right) of osteoblasts of adult female B6 mice, wild-type littermates of *ob/ob* mice (WT ob$^+$/ob$^+$), or *ob/ob* (ob$^-$/ob$^-$) mice. In left, Results are shown as the % of respective static cells (mean ± SD, n = 3). *p<0.05 vs. static control, and #p<0.05 vs. the B6 and WT ob/ob cells. In right, the top lane was a representative blot of pErk1 and pErk2 using an anti-pErk1/2 antibody. The bottom lane was a representative blot of total Erk1/2 identified by an anti-pan Erk antibody.

Lepr is a member of the class I cytokine receptor family and uses the Jak2/Stat 3 pathway as its primary signaling pathway. Thus, we measured the relative levels of protein-tyrosine phosphorylated (pY-)Jak2/Jak2 and pY-Stat3/Stat3 as an index of activation of the *Lepr* signaling, in C3H/HeJ and C57BL/6J osteoblasts without (basal) or with the fluid shear. Osteoblasts of *ob*$^-$/*ob*$^-$ mice were included in this experiment for comparison. To ensure full activation of the *Lepr* signaling, the cells were pre-treated with 100 ng/ml leptin for 24 hrs prior to the shear stress. **Figure 16A** shows that the basal leptin-dependent increases in pY-Jak2 and pY-Stat3 levels were much higher in the C3H/HeJ osteoblasts than those in C57BL/6J and *ob*$^-$/*ob*$^-$ osteoblasts, suggesting that C3H/HeJ osteoblasts have a functionally more active *Lepr* signaling. **Figure 16B** also shows that shear stress reduced the relative amounts of pY-Jak2 and pY-Stat3 in all three osteoblasts, suggesting that fluid shear stress may have suppressive effects on the *Lepr* signaling in mouse osteoblasts.

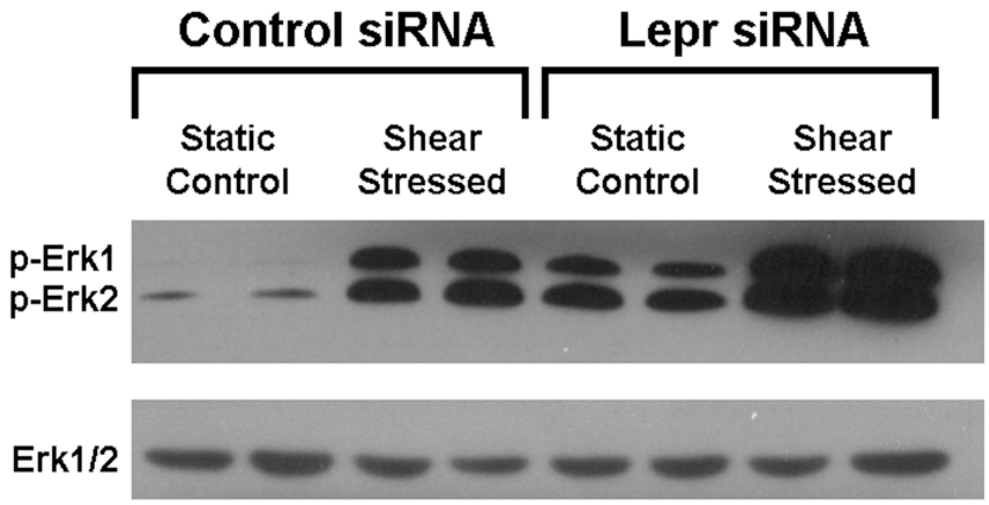

Figure 15: siRNA-mediated suppression of *Lepr* expression enhanced basal and shear stress-induced Erk1/2 phosphorylation in C57BL6/J osteoblasts. Total Erk1/2 was measured with an anti-pan-Erk antibody.

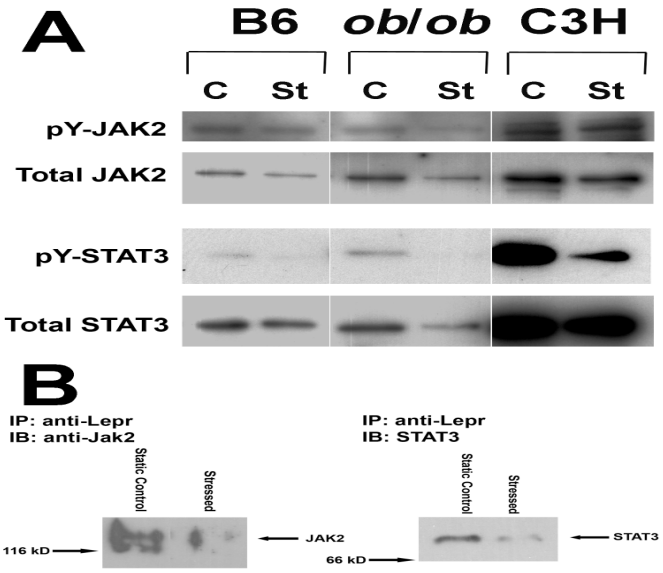

Figure 16: Effects of fluid shear stress on leptin-mediated induced phosphorylation of JAK2 and STAT3 (A) and on the amounts of co-immunoprecipitated Jak2 and Stat3 with Lepr in B6 osteoblasts (B). In A, primary osteoblasts isolated from B6, *ob*-/*ob*-, and C3H mice were each treated with 100 ng/ml leptin with or without the 30-min steady fluid shear stress of 20 dynes/cm2. Ten minutes after the shear stress, the stressed cells (St) and the corresponding static control cells (C) were lysed in RIPA, and the relative levels of pY-Jak2 and total Jak2 as well as those of pY-Stat3 and total Stat3 were analyzed by Western blot. In B, immediately after the 30-min shear stress, cell extracts of the stressed and static control B6 osteoblasts were immunoprecipitated (IP) with anti-Lepr and blotted (IB) against anti-Jak2 (left panel) or anti-Stat3 (right panel).

It is interesting that the total Jak2 and Stat3 levels were several folds higher in C3H osteoblasts than in C57BL/6J and *ob*$^{-}$/*ob*$^{-}$ osteoblasts. Thus, inasmuch as the fluid shear suppressed the leptin-mediated pY-Jak2 and pY-Stat3 levels in C3H/HeJ osteoblasts, the remaining pY-Jak2 and pY-Stat3 levels in C3H/HeJ osteoblasts were still several folds higher than basal pY-Jak2 and pY-Stat3 levels in B6 and *ob*$^{-}$/*ob*$^{-}$ osteoblasts.

Other members of the class I cytokine receptor family could also activate the Jak2/Stat3 signaling. To ensure that the fluid shear-mediated reduction in the Jak2/Stat3 activation was related to the *Lepr* signaling, we performed a co-immunoprecipitation experiment to assess the relative amounts of Lepr-associated Jak2/Stat3 in B6 osteoblasts (Fig. 16B). The fluid shear reduced markedly the amounts of Lepr-bound Jak2 and Stat3; a finding consistent with the contention that the reduced Jak2/Stat3 activation was related to the shear stress-mediated reduction in the *Lepr* signaling.

In studies with respect to the role of IGF-I signaling in mechanotransduction involving protein-tyrosine phosphorylation, we are now using a knock out approach, which has demonstrated that osteoblast derived IGF-I is critical in mediating skeletal anabolic response to mechanical loading. The next phase of our study is to identify the genes and the signaling pathways that are down stream of IGF-I involved in increasing the bone formation in response to mechanical loading. To do so, we generated IGF-I KO and littermate wild type mice. At 5 weeks of age, these mice were euthanized and tibias were collected, marrow flushed and stored in DMEM+ antibiotic tube. Later, to harvest primary osteoblast cells, these bones were chopped and incubated at 37ºC for 2 hour with 0.1% collagenase. After the incubation, supernatant were discarded and cells were collected and transferred to a culture plate that contains 10% FBS, antibiotics and DMEM. Currently we are setting up the fluid flow stress to perform in vitro mechanical stimulation on the collected primary osteoblast cells from both KO and wild type mice. Once mechanical stimulation is completed, protein will be extracted from the mechanical stimulated vs. non-stimulated cell and western blot approach will be used to evaluate signaling proteins that are increased in response to mechanical loading. The findings of this study will be reported in our next progress report.

Technical Objective 7: **Continue data analysis and prepare manuscripts for submission to peer review journals for publication**

We have submitted a manuscript on our results of the potential role of leptin receptor as a negative regulator of mechanosensitivity (The leptin receptor signaling functions as a negative modulator of bone mechnosensitivity in mice) for publication in the Journal of Biological Chemistry. This manuscript has been reviewed and is potentially acceptable for publication upon appropriate revision. We are now in the process of revising the manuscript for resubmission.

We have completed the data analysis for the previous bone termination study and have communicated to peer review journal. Currently, we are organizing the data generated from IGF-I KO mice.

Technical Objective 8: **Prepare final progress report for submission to TATRC**. This technical objective will be completed during the remainder of the no-cost extension period.

Key Findings

1. Mechanical loading by four-point bending in the mid-diaphysis produced osteogenic response in the wild type mice but not in the conditional IGF-I KO mice.
2. Axial loading of tibia increased both cortical and trabecular BMD in the wild type mice but not in the conditional IGF-I KO mice.
3. Mechanical loading-induced increase in Runx2 expression failed to occur in the IGF-I KO mice, thus suggesting IGF-I is essential for mechanical loading-induced increase in Runx2 expression.
4. Mechanical loading-induced increases in bone density and bone size were not any different between the Formin-2 KO and wild type mice.
5. *Our in vitro* data together with the *in vivo* loading data demonstrate that deficiency of leptin expression or *Lepr* signaling enhanced the osteogenic response to mechanical stimulation
6. Several potential functional candidates in the mutant locus of 14104M did not show mutation in the coding region.

Conclusions

1) Osteoblast produced IGF-I is essential for the mechanical loading-induced increase in new bone formation, thus suggesting that other growth factors cannot compensate for the lack of local IGF-I to produce skeletal anabolic response to mechanical loading.
2) Formin-2 KO study proves that this gene is not a major mediator of skeletal anabolic response to loading.
3) Our sequencing studies of functional positional candidates in the 14104M mutant locus reveal that 14104M gene is a novel gene that regulates bone size.
4) Our in vivo and in vitro findings demonstrate that leptin signaling is an important negative regulator of mechanical loading response.

Reportable Outcomes

1. Oral presentation at 30th meeting of ASBMR for the paper entitled "Conditional Disruption of IGF-I Gene in Osteoblasts Demonstrates Obligatory and Non-Redundant Role of IGF-I in Skeletal Anabolic Response to Mechanical Loading, 2009.
2. Kesavan Chandrasekhar and Subburaman Mohan. Bone mass gained in response to external loading is lost following cessation of loading in 10 week C57BL/6J mice.

Manuscript communicated to *Biomechanics and Modeling in Mechanobiology*, waiting for reply 2009.

References:

1. Gullberg B, Johnell O, Kanis JA 1997 World-wide projections for hip fracture. Osteoporos Int 7(5):407-13.
2. Akhter MP, Cullen DM, Pedersen EA, Kimmel DB, Recker RR 1998 Bone response to in vivo mechanical loading in two breeds of mice. Calcif Tissue Int 63(5):442-9.
3. Umemura Y, Baylink DJ, Wergedal JE, Mohan S, Srivastava AK 2002 A time course of bone response to jump exercise in C57BL/6J mice. J Bone Miner Metab 20(4):209-15.
4. Kesavan C, Mohan S, Oberholtzer S, Wergedal JE, Baylink DJ 2005 Mechanical loading-induced gene expression and BMD changes are different in two inbred mouse strains. J Appl Physiol 99(5):1951-7.
5. Bikle DD, Sakata T, Halloran BP 2003 The impact of skeletal unloading on bone formation. Gravit Space Biol Bull 16(2):45-54.
6. Lau KH, Kapur S, Kesavan C, Baylink DJ 2006 Up-regulation of the Wnt, estrogen receptor, insulin-like growth factor-I, and bone morphogenetic protein pathways in C57BL/6J osteoblasts as opposed to C3H/HeJ osteoblasts in part contributes to the differential anabolic response to fluid shear. J Biol Chem 281(14):9576-88.
7. Kapur S, Mohan S, Baylink DJ, Lau KH 2005 Fluid shear stress synergizes with insulin-like growth factor-I (IGF-I) on osteoblast proliferation through integrin-dependent activation of IGF-I mitogenic signaling pathway. J Biol Chem 280(20):20163-70.
8. Kapur S, Chen ST, Baylink DJ, Lau KH 2004 Extracellular signal-regulated kinase-1 and -2 are both essential for the shear stress-induced human osteoblast proliferation. Bone 35(2):525-34.
9. Boutahar N, Guignandon A, Vico L, Lafage-Proust MH 2004 Mechanical strain on osteoblasts activates autophosphorylation of focal adhesion kinase and proline-rich tyrosine kinase 2 tyrosine sites involved in ERK activation. J Biol Chem 279(29):30588-99.
10. Liedert A, Kaspar D, Blakytny R, Claes L, Ignatius A 2006 Signal transduction pathways involved in mechanotransduction in bone cells. Biochem Biophys Res Commun 349(1):1-5.
11. Kunnel JG, Igarashi K, Gilbert JL, Stern PH 2004 Bone anabolic responses to mechanical load in vitro involve COX-2 and constitutive NOS. Connect Tissue Res 45(1):40-9.
12. Danciu TE, Adam RM, Naruse K, Freeman MR, Hauschka PV 2003 Calcium regulates the PI3K-Akt pathway in stretched osteoblasts. FEBS Lett 536(1-3):193-7.
13. Kesavan C, Mohan S, Srivastava AK, Kapoor S, Wergedal JE, Yu H, Baylink DJ 2006 Identification of genetic loci that regulate bone adaptive response to mechanical loading in C57BL/6J and C3H/HeJ mice intercross. Bone Sep;39(3):634-43.
14. Kesavan C, Baylink DJ, Kapoor S, Mohan S 2007 Novel loci regulating bone anabolic response to loading: expression QTL analysis in C57BL/6JXC3H/HeJ mice cross Bone Aug;41(2):223-30.
15. De Souza RL, Matsuura M, Eckstein F, Rawlinson SC, Lanyon LE, Pitsillides AA 2005 Non-invasive axial loading of mouse tibiae increases cortical bone formation and modifies

trabecular organization: a new model to study cortical and cancellous compartments in a single loaded element. Bone 37(6):810-8.

16. Sugiyama T, Saxon LK, Zaman G, Moustafa A, Sunters A, Price JS, Lanyon LE 2008 Mechanical loading enhances the anabolic effects of intermittent parathyroid hormone (1-34) on trabecular and cortical bone in mice. Bone 43(2):238-48.
17. Ohashi N, Robling AG, Burr DB, Turner CH 2002 The effects of dynamic axial loading on the rat growth plate. J Bone Miner Res 17(2):284-92.
18. Alam I, Warden SJ, Robling AG, Turner CH 2005 Mechanotransduction in bone does not require a functional cyclooxygenase-2 (COX-2) gene. J Bone Miner Res 20(3):438-46.
19. Warden SJ, Turner CH 2004 Mechanotransduction in the cortical bone is most efficient at loading frequencies of 5-10 Hz. Bone 34(2):261-70.
20. Srinivasan S, Weimer DA, Agans SC, Bain SD, Gross TS 2002 Low-magnitude mechanical loading becomes osteogenic when rest is inserted between each load cycle. J Bone Miner Res 17(9):1613-20.
21. Xing W, Baylink D, Kesavan C, Hu Y, Kapoor S, Chadwick RB, Mohan S 2005 Global gene expression analysis in the bones reveals involvement of several novel genes and pathways in mediating an anabolic response of mechanical loading in mice. J Cell Biochem 96(5):1049-60.
22. Mohan S, Baylink DJ, Srivastava AK. 2007 A chemical mutagenesis screen to identify modifier genes that interact with growth hormone and TGF-beta signaling pathways. Bone. 2008 Feb;42(2):388-95.
23. Srivastava AK, Kapur S, Mohan S, Yu H, Kapur S, Wergedal J, Baylink DJ. 2005 Identification of novel genetic loci for bone size and mechanosensitivity in an ENU mutant exhibiting decreased bone size. J Bone Miner Res Jun; 20(6):1041-50.
24. Mohan S, Chest V, Chadwick RB, Wergedal JE, Srivastava AK. 2007 Chemical mutagenesis induced two high bone density mouse mutants map to a concordant distal chromosome 4 locus. Bone Nov; 41(5):860-8.
25. Wheeler HE, Metter EJ, Tanaka T, Absher D, Higgins J, Zahn JM, Wilhelmy J, Davis RW, Singleton A, Myers RM, Ferrucci L, Kim SK 2009 Sequential use of transcriptional profiling, expression quantitative trait mapping, and gene association implicates MMP20 in human kidney aging. PLoS Genet. 2009 Oct; 5(10):e1000685.
26. Umeno J, Matsumoto T, Esaki M, Kukita Y, Tahira T, Yanaru-Fujisawa R, Nakamura S, Arima H, Hirahashi M, Hayashi K, Iida M. 2009 Impact of group IVA cytosolic phospholipase A (2) gene polymorphisms on phenotypic features of patients with familial adenomatous polyposis. Int J Colorectal Dis. Oct 1.
27. Edvardson S, Hama H, Shaag A, Gomori JM, Berger I, Soffer D, Korman SH, Taustein I, Saada A, Elpeleg O 2008 Mutations in the fatty acid 2-hydroxylase gene are associated with leukodystrophy with spastic paraparesis and dystonia. Am J Hum Genet Nov;83(5):643-8.
28. Edderkaoui B, Baylink DJ, Beamer WG, Wergedal JE, Porte R, Chaudhuri A, Mohan S 2007 Identification of mouse Duffy antigen receptor for chemokines (Darc) as a BMD QTL gene. Genome Res May; 17(5):577-85.

29. Meyer-Lindenberg A, Nichols T, Callicott JH, Ding J, Kolachana B, Buckholtz J, Mattay VS, Egan M, Weinberger DR 2006 Impact of complex genetic variation in COMT on human brain function. Mol Psychiatry Sep; 11(9):867-77, 797.

APPENDIX 1

Oral presentation at 30th meeting of ASBMR for the paper entitled "Conditional Disruption of IGF-I Gene in Osteoblasts Demonstrates Obligatory and Non-Redundant Role of IGF-I in Skeletal Anabolic Response to Mechanical Loading, 2009.

Conditional Disruption of IGF-I Gene in Osteoblasts Demonstrates Obligatory and Non-Redundant Role of IGF-I in Skeletal Anabolic Response to Mechanical Loading. C. Kesavan*, J. Wergedal, S. Mohan. JLP VA Med Ctr and Loma Linda Univ, Loma Linda, CA 92357, USA.

Although a key role for mechanical stress (MS) in the development of skeletal architecture and in the maintenance of bone mass is well established, little is known about the genes and their signaling pathways that contribute to MS response in bone in vivo. Based on the findings that the expression of IGF-I, a key bone formation (BF) regulator, increases rapidly in response to MS in osteoblasts (OBs) *in vitro* and *in vivo*, we proposed the hypothesis that OB produced IGF-I is the key mediator of skeletal anabolic response to MS. To test the cause and effect relationship of OB produced IGF-I and skeletal anabolic response to mechanical loading (ML), we generated mice with conditional disruption of IGF-I in OBs using Cre/loxP technology. In our initial study, a 4-point bending device was used to apply daily a load to the mid diaphysis of tibia of 10-wk old mice at a frequency of 2Hz for 36 cycles for a period of 2 weeks. Because bone size was smaller in the knockout (KO) compared to wild type (WT) mice, the load was adjusted such that the applied load produced equivalent amount of strain in both KO and WT mice. Measurement of skeletal changes by pQCT revealed that two weeks of ML caused a robust 10% ($P<0.05$) and 39% ($P<0.01$) increases in BMD and cross sectional area (CSA), respectively, in the WT mice. However, application of the same amount of strain to KO mice did not significantly increase either BMD (3.2%) or CSA (3%). Accordingly, expression levels of BSP (2.4 fold, $P<0.01$) and runx2 (2.1 fold, $P=0.05$) as measured by real time RT-PCR were increased significantly in response to ML in the WT but not KO mice. To determine if OB-produced IGF-I is also necessary for ML-induced changes in trabecular bone, we next used tibial axial loading model to apply 12N in WT and 6.5 N in KO of axial load to generate 825 and 747με strain, respectively, in the WT and KO mice at 10 weeks of age. Micro-CT analyses of newly formed trabecular bone at secondary spongiosa, at 10.5μ resolution, revealed 23%, 19% and 21% (all $P<0.05$) increases in trabecular BV/TV, thickness and density in the loaded bones of WT mice compared to corresponding non-loaded bones. In contrast, trabecular bone parameters, if any, were decreased in the loaded bones of KO mice. We conclude that OB produced IGF-I is obligatory for the ML-induced increase in new BF, thus suggesting that other growth factors cannot compensate for lack of local IGF-I to produce skeletal anabolic response to ML.

Editorial Manager(tm) for Biomechanics and Modeling in Mechanobiology
Manuscript Draft

Manuscript Number: BMMB-09-336

Title: Bone mass gained in response to external loading is lost following cessation of loading in 10 week C57BL/6J mice

Article Type: Short Communication

Keywords: density, bone fate, physical exercise, rehabilitation, Mice

Corresponding Author: Dr. Subburaman Mohan, Ph.D.

Corresponding Author's Institution: JL Pettis VA Mem Med Ctr

First Author: Chandrasekhar Kesavan, Ph.D.

Order of Authors: Chandrasekhar Kesavan, Ph.D.; Subburaman Mohan, Ph.D.

Abstract: Dynamic loads lead to increases in bone mass. How long these gains are maintained after cessation of loading, however, is not fully understood. To address this, a long term study was performed in which skeletal changes were monitored every 2-4 weeks for a 12 week period following application of external loading to the right tibia of 10 week old female C57BL/6J mice. 2 weeks of loading caused a drastic 40% increase in cross sectional area (CSA) and 15% increase in total vBMD as measured by pQCT. Accordingly, the bone parameters related to bone strength (yield load, maximum load and toughness) were also increased (29-42%) significantly when compared to non-externally loaded bones. Presence of significant correlations between bone parameters and mechanical properties ($r=0.72$ to 0.88, $p<0.05$) suggest that the changes in bone parameters induced by loading are responsible, in part, for the increase in bone strength after the last loading. However, cessation of loading resulted in a continuous loss of BMD and CSA as well as bone strength. The vBMD returned to normal at 12 weeks with a half life of 6 weeks and CSA declined with a half life of 8.5 weeks and was still elevated at 12 weeks. Our results show that external loading increased bone mass temporarily and that periodic loading maybe necessary to maintain long term bone strength.

Bone mass gained in response to external loading is lost following cessation of loading in 10 week C57BL/6J mice

Chandrasekhar Kesavan and Subburaman Mohan

[1]Chandrasekhar Kesavan
Musculoskeletal Disease Center, VA Loma Linda Healthcare System, Loma Linda, CA 92357.
Email: Chandrasekhar.Kesavan@va.gov

[2]Subburaman Mohan
Musculoskeletal Disease Center (151), VA Loma Linda Health Care System, Loma Linda, CA 92357.
Department of Medicine, Physiology and Biochemistry, Loma Linda University, Loma Linda, CA 92354.
Email: Subburaman.Mohan@va.gov

Address correspondence:
Subburaman Mohan, Ph.D
Musculoskeletal Disease Center (151),
Jerry L. Pettis Memorial VA Medical Center,
11201 Benton Street, Loma Linda, CA 92357.
Email: Subburaman.Mohan@va.gov,
Ph: 909-825-7084 Extension: 2932
Fax: 909-796-1680

Abstract

Dynamic loads lead to increases in bone mass. How long these gains are maintained after cessation of loading, however, is not fully understood. To address this, a long term study was performed in which skeletal changes were monitored every 2-4 weeks for a 12 week period following application of external loading to the right tibia of 10 week old female C57BL/6J mice. 2 weeks of loading caused a drastic 40% increase in cross sectional area (CSA) and 15% increase in total vBMD as measured by pQCT. Accordingly, the bone parameters related to bone strength (yield load, maximum load and toughness) were also increased (29-42%) significantly when compared to non-externally loaded bones. Presence of significant correlations between bone parameters and mechanical properties ($r=0.72$ to 0.88, $p<0.05$) suggest that the changes in bone parameters induced by loading are responsible, in part, for the increase in bone strength after the last loading. However, cessation of loading resulted in a continuous loss of BMD and CSA as well as bone strength. The vBMD returned to normal at 12 weeks with a half life of 6 weeks and CSA declined with a half life of 8.5 weeks and was still elevated at 12 weeks. Our results show that external loading increased bone mass temporarily and that periodic loading maybe necessary to maintain long term bone strength.

Key words: density, bone fate, physical exercise, rehabilitation, Mice

1 Introduction

It is now well established that mechanical loading is an effective stimulator of bone formation. Past studies using animal and human models have shown that loading increases bone formation while non-loading, such as prolonged bed rest, immobilization, and space flight, results in increase in bone loss (Bailey & McCulloch, 1990; Akhter et al., 1998; Kesavan et al., 2005; Kodama et al., 2000; Lang et al., 2006; Mori et al., 2003; Turner & Robling, 2004; Bikle & Halloran, 1999; Bikle et al., 2003). We, and others, using inbred strains of mice, have reported that mechanical loading causes increases in the bone mineral density (BMD) when measured by peripheral quantitative computed tomography (pQCT) (Kesavan et al., 2005; Akhter et al., 1998). Thus, physical exercise has been used as a strategy to maintain BMD and prevent osteoporotic fractures in men and women.

Recent clinical studies in young and postmenopausal women who were subjected to treadmill exercise have shown that exercise induced benefits, such as increases in BMD and bone mineral content (BMC), are eventually lost if exercise is ceased completely (Dalsky et al., 1988). Similar data was presented by Vuori *et al*. when reporting that unilateral leg presses done four times a week for 12 months increased bone mass (BMD) but returned to pre-training levels with only 3 months of retirement from exercise (Vuori et al., 1994; Karlsson, 2003). Data from various independent studies in humans suggest that exercise induced bone mass benefits seem to be eroded by time. Animal studies using rat model have shown that increased femoral BMD, gained through treadmill exercise, resulted in decreased bone formation rate after deconditioning

(Iwamoto et al., 2000; Pajamaki et al., 2003). We, and others, have previously shown that C57BL/6J (B6), a low bone density mouse, responds well to mechanical loading. We have reported that 2 weeks of mechanical loading by four-point bending causes a 10-15% increase in tibia BMD and 30-40% increase in cross-sectional area in 10 week old female B6 mice (Kesavan et al., 2005). We have extended this study further to examine how long this newly formed bone, induced by four-point bending, is maintained and its fate after cessation of loading, using the good responder, B6 mouse.

2 Materials and methods

Mice

Female C57BL/6J were purchased from the Jackson Laboratory (Bar Harbor, Me). All mice were housed under the standard conditions of 14-hour light and 10-hour darkness, and had free access to food and water. The body weights of these animals measured before the initial loading were 18.32 ± 0.79 grams. The experimental protocols were in compliance with animal welfare regulations and approved by our local IACUC.

In vivo loading model/ regimen

At 10 weeks of age the mice were subjected to mechanical loading using the four-point bending device as described previously (Kesavan et al., 2005). The loading protocol consists of a 9.0 Newton (N) force at a frequency of 2 Hz for 36 cycles, performed daily under inhalable anesthesia (5% Halothane and 95% oxygen). The loading procedure was repeated for 6 days/week with 1 day of rest for 2 weeks. The right tibia (externally loaded bone) was used for loading and the left tibia (non-externally loaded bone) as internal

control in each mouse. A schematic representation of the study design is shown in Figure.1

Peripheral quantitative computed tomography (pQCT) measurements

To measure loading induced changes in bone parameters in the externally loaded and contralateral control tibia, we used pQCT (Stratec XCT 960M, Norland Medical System, Ft. Atkinson, WI) as described previously (Kesavan et al., 2005; Kesavan et al., 2006). *In vivo* pQCT measurements were performed at 0, 2, 4, 6, 8, and 12 weeks after the last loading regimen.

Mechanical properties of bone

Tibiae were stored frozen in gauze moistened with PBS and thawed in PBS at 4°C. The anterior-posterior diameter (AP.Dm) and lateral-medial diameter (LM.Dm) were measured with calipers. The tibiae were tested in three-point bending using the Instron DynaMight testing system (Model 8840; Instron, Canton, MA, USA) as previously described (Wergedal et al., 2002). Each tibia was placed on two immovable supports which were 5 mm apart. An initial 1.0 N was applied on the tibia at a position of 2.10 mm away from the tibia-fibular junction to prevent the rotation of the bone due to the shape of tibia and to be consistent in breaking region between the bones. Furthermore, this area corresponds to the 4 mm loading region. It was then loaded from this midpoint at a constant rate (2 mm/minute) to the point of fracture. Load displacement curves were used to calculate yield load (P_y), maximum load (P_{max}) and toughness (Ut). Cross sectional moment of inertia was calculated from the measured anterior-posterior Dm and

lateral-medial Dm and from the average cortical thickness obtained by pQCT analysis as previously described (Wergedal et al., 2006).

Statistical analysis

Data are presented as Mean ± Standard error (SE). Loading induced changes in skeletal parameters were determined by calculating percent changes in the externally loaded bone versus non-externally loaded bone of the same animal to avoid any inherent variation between animals. Regression analysis and standard t-test were used to compare loading induced skeletal changes. We used STATISTICA software (StatSoft, Inc version 7.1, 2005) for our analysis and the results were considered significantly different at $p<0.05$.

3 Results

Bone anabolic response after cessation of loading

Two weeks of mechanical loading by four-point bending increased bone mineral content (BMC) by 45% in the loaded bone compared to corresponding non-externally loaded bone. The increased BMC was maintained (10-45%) throughout the 12 week cessation period after last loading (Fig.2A). The increased BMC in the loaded bone is caused by both bone size and BMD changes. Bone size, as reflected by periosteal circumference was increased by 18% after two weeks of mechanical loading and was significantly different from corresponding non-externally loaded bone throughout the entire study (Fig.2B). vBMD was increased by 14% after two weeks of mechanical loading and remained high only until 4 weeks after cessation of exercise (Fig.2C).

Figure 3 shows loss rate of loading-induced increases in bone size and BMD as a function of time after cessation of last loading. Both cross sectional area (CSA) and BMD were lost with time but at different rates. The pQCT images of externally loaded and non-externally loaded bones immediately after last loading and 8 weeks after cessation of loading reveal that much of the newly formed bone at the loaded site is lost at the end of experimental period (Fig.4).

Bone mechanical properties after termination of loading

To determine, if loading induced changes in bone parameters reflect an increase or decrease in mechanical properties of bone, we performed a bone breaking study at 0 time and at 12 weeks after cessation of last loading by using a three-point bending device. We found that immediately after 2 weeks of loading yield load, maximum load and toughness were significantly increased by 42%, 29% and 42%, respectively in the externally loaded bones compared to non-externally loaded bones (Table 1). However, at 12 weeks, there was no difference in these parameters between externally loaded and non-externally loaded bones (Table 1).

4 Discussion

In this study, the choice of inbred strain of mice, the loading device and regimen used were chosen based on previous findings (Kesavan et al., 2006; Kesavan et al., 2005). Two weeks of four-point bending on the right tibiae when compared to left tibiae resulted in a significant increase in bone parameters, such as BMC, CSA and BMD, as

shown in Figure.2. The magnitude of increase in skeletal parameters after 2 weeks of loading is consistent with our previous study (Kesavan et al., 2005). However, in this study, we show that this increase in CSA and BMD gained immediately after loading did not continue over time after the cessation of last external loading. This is because BMD increased with age in non-externally loaded tibiae but not in the externally loaded tibiae and as such the difference in BMD between externally loaded and non-externally loaded bones was lost 4 wks after cessation of loading (Fig.2). This suggests that bone anabolic response does not continue once loading is terminated.

We also found that the loading induced a 15% and 40% increase in BMD and CSA, respectively, immediately after 2 weeks of four-point bending (Fig.3). However, cessation of loading resulted in a continuous loss of both BMD and CSA. We found that the loading induced changes in volumetric BMD returned to normal at 12 weeks with a half life of 6-weeks. The change in CSA declined with a half life of 8.5 weeks and was still significantly elevated at 12 weeks. Thus, the decline in elevated CSA proceeded at a much slower pace than the loading induced increase in vBMD.

In the pQCT analysis of bone parameters using the lower threshold (180-730), we found that the magnitude of increase in periosteal circumference (PC) was 18% ± 7.0 after the last loading and was very significant when compared with 7.2% ± 1.7 using the higher threshold (730-730). This is due to rapid accumulation of less mineralized bone at the periosteal surface. This is most prevalent at 0 time point (immediately after the last loading), as seen by the red color using the pQCT threshold indicator (Fig.4).

Consequently, we found a significant increase in CSA at 0 time point, accompanied by an increase in BMD. Over time, we found that periosteal circumference increased with age in the non-externally loaded but not the externally loaded tibia. As a result, the magnitude of difference between externally loaded and non-externally loaded tibia decreased with time after cessation of loading, resulting in no difference in the periosteal circumference of externally loaded tibia between lower (PC, 9.13% ± 3.9) and higher threshold (PC, 9.8% ± 1.2). These findings, suggest that the newly formed bone undergoes remodeling at the periosteal site to cortical bone over time which leads to a reduction in bone size in order to accommodate the loading induced changes in the bone shape. During this remodeling process, we found that the rate of loss in gained CSA (bone size) after cessation of loading was 10% every 2 weeks for 8 weeks. These data, together, suggest that the positive effects of mechanical loading on CSA were maintained for several weeks after the cessation of last external loading.

In this study, we observed that the accommodation of this newly formed bone, gained through loading, altered the shape of bone over time compared with non-externally loaded tibia as seen from our pQCT cross-sectional slices. Since studies have shown that increase in bone parameters lead to an increase in bone mechanical properties, one would expect measurable differences in mechanical properties between the bones immediately after loading and 12 weeks later. To test this, we measured yield load, maximum load and toughness in both externally loaded and non-externally loaded tibiae using the three-point bending device. The results from our study show a significant increase in the bone strength immediately after 2- weeks of loading in the externally

loaded bones compared to non-externally loaded bones, as evident from data shown in Table 1. In order to determine if the increase in bone mechanical properties is due to an increase in the changes in bone parameters, measured by pQCT, we performed correlation analysis between BMD, CSA, cortical thickness and mechanical properties of bone. The results show a significant correlation between BMD, area and cortical thickness with yield load, maximum load and toughness ($r = 0.72$ to 0.88, $p<0.05$). These data suggest that the changes in bone parameters induced by mechanical loading are responsible, in part, for the increase in bone strength at 0 time point. However, this increase in bone strength was lost at 12 weeks. Accordingly, we found that there was no difference in the yield load, maximum load and toughness between the externally loaded and non-externally loaded bones (Table 1) at 12 weeks after the cessation of loading. This is consistent with the loss of loading induced changes in bone parameters. Together, our findings indicate that the external loading-induced increases in bone are lost over a period of time but at a much slower pace than the induction of the increases. It is worth mentioning that reports by others have predicted that some of the skeletal changes induced by four-point bending are due to periosteal pressure. In our previous QTL study, we have found that sham-loading neither increased periosteal bone formation nor caused changes in expression levels of bone marker genes, demonstrating that the skeletal changes induced by bending are not due to periosteal pressure (Kesavan et al., 2006). This finding also applies to the present study since we used the same loading model as well as regimen. In conclusion, our study shows that a single burst of external loading provides increased bone mass temporarily, periodic loading may be necessary to maintain long term bone strength.

ACKNOWLEDGEMENTS

This work was supported by the Army Assistance Award No. DAMD17-01-1-744. The US Army Medical Research Acquisition Activity (Fort Detrick, MD) 21702-5014 is the awarding and administering acquisition office for the DAMD award. The information contained in this publication does not necessarily reflect the position or the policy of the Government, and no official endorsement should be inferred. All work was performed in facilities provided by the Department of Veterans Affairs. We would like to thank Mr. James Dekeyser for his technical support in four-point bending instrument and Peter Gifford for the animal work.

Fig.1 A schematic representation of the study design.

Fig.2 Changes in bone parameters measured at different time points after cessation of loading.
The y-axis corresponds to absolute changes in bone parameters in response to 12 days four-point bending on 10 week female C57BL/6J mice. The x-axis corresponds to various time points. (A) Bone mineral content (BMC), (B) Periosteal circumference (PC) and (C) Bone mineral Density (BMD). Values are mean ± SE, *$p<0.05$ vs. non-externally loaded tibiae, N=5.

Fig.3 Changes in CSA and BMD measured at different time points after cessation of loading.
The y-axis corresponds to percent change and x-axis corresponds to duration (weeks). CSA, Cross sectional area and vBMD, total volumetric bone mineral density, values are mean ± SE, *$p<0.05$ vs. non-externally loaded tibiae, N=5.

Fig.4 Cross sectional area of the externally loaded tibia vs. non-externally loaded tibia.
This figure shows the newly formed bone at the periosteal site in response to 2 weeks loading and its fate over time after cessation of loading. The arrow corresponds to newly formed bone and the white color represents cortical bone.

REFERENCES:

Akhter MP, Cullen DM, Pedersen EA, Kimmel DB, Recker RR (1998) Bone response to in vivo mechanical loading in two breeds of mice. Calcif Tissue Int 63:442-449.

Bailey DA, McCulloch RG (1990) Bone tissue and physical activity. Can J Sport Sci 15:229-239.

Bikle DD, Halloran BP (1999) The response of bone to unloading. J Bone Miner Metab 17:233-244.

Bikle DD, Sakata T, Halloran BP (2003) The impact of skeletal unloading on bone formation. Gravit Space Biol Bull 16:45-54.

Dalsky GP, Stocke KS, Ehsani AA, Slatopolsky E, Lee WC, Birge SJ Jr. (1988) Weight-bearing exercise training and lumbar bone mineral content in postmenopausal women. Ann Intern Med 108:824-828.

Iwamoto J, Yeh JK, Aloia JF (2000) Effect of deconditioning on cortical and cancellous bone growth in the exercise trained young rats. J Bone Miner Res 15:1842-1849.

Karlsson MK (2003) The skeleton in a long-term perspective--are exercise induced benefits eroded by time? J Musculoskelet Neuronal Interact 3:348-351; discussion 356.

Kesavan C, Mohan S, Oberholtzer S, Wergedal JE, Baylink DJ (2005) Mechanical loading-induced gene expression and BMD changes are different in two inbred mouse strains. J Appl Physiol: 99:1951-1957.

Kesavan C, Mohan S, Srivastava AK, Kapoor S, Wergedal JE, Yu H, Baylink D J (2006) Identification of genetic loci that regulate bone adaptive response to mechanical loading in C57BL/6J and C3H/HeJ mice intercross. Bone 39:634-643.

Kodama Y, Umemura Y, Nagasawa S, Beamer WG, Donahue LR, Rosen CR, Baylink DJ, Farley JR (2000) Exercise and mechanical loading increase periosteal bone formation and whole bone strength in C57BL/6J mice but not in C3H/Hej mice. Calcif Tissue Int 66:298-306.

Lang TF, Leblanc AD, Evans HJ, Lu Y (2006) Adaptation of the proximal femur to skeletal reloading after long-duration spaceflight. J Bone Miner Res 21:1224-1230.

Mori T, Okimoto N, Sakai A, Okazaki Y, Nakura N, Notomi T, Nakamura T (2003) Climbing exercise increases bone mass and trabecular bone turnover through transient regulation of marrow osteogenic and osteoclastogenic potentials in mice. J Bone Miner Res 18: 2002-2009.

Pajamaki I, Kannus P, Vuohelainen T, Sievanen H, Tuukkanen J, Jarvinen M, Jarvinen TL (2003) The bone gain induced by exercise in puberty is not preserved through a virtually life-long deconditioning: a randomized controlled experimental study in male rats. J Bone Miner Res 18:544-52.

Turner CH, Robling AG (2004) Exercise as an anabolic stimulus for bone. Curr Pharm Des 10:2629-2641.

Vuori I, Heinonen A, Sievanen H, Kannus P, Pasanen M, Oja P (1994) Effects of unilateral strength training and detraining on bone mineral density and content in young women: a study of mechanical loading and deloading on human bones. Calcif Tissue Int 55:59-67.

Wergedal JE, Ackert-Bicknell CL, Tsaih SW, Sheng MH, Li R, Mohan S, Beamer WG, Churchill GA, Baylink, DJ (2006) Femur mechanical properties in the F2 progeny of an NZB/B1NJ x RF/J cross are regulated predominantly by genetic loci that regulate bone geometry. J Bone Miner Res 21:1256-1266.

Wergedal JE, Sheng MH, Ackert-Bicknell CL, Beamer WG, Baylink DJ (2002) Mouse genetic model for bone strength and size phenotypes: NZB/B1NJ and RF/J inbred strains. Bone 31:670-4.

Fig1

Click here to download high resolution image

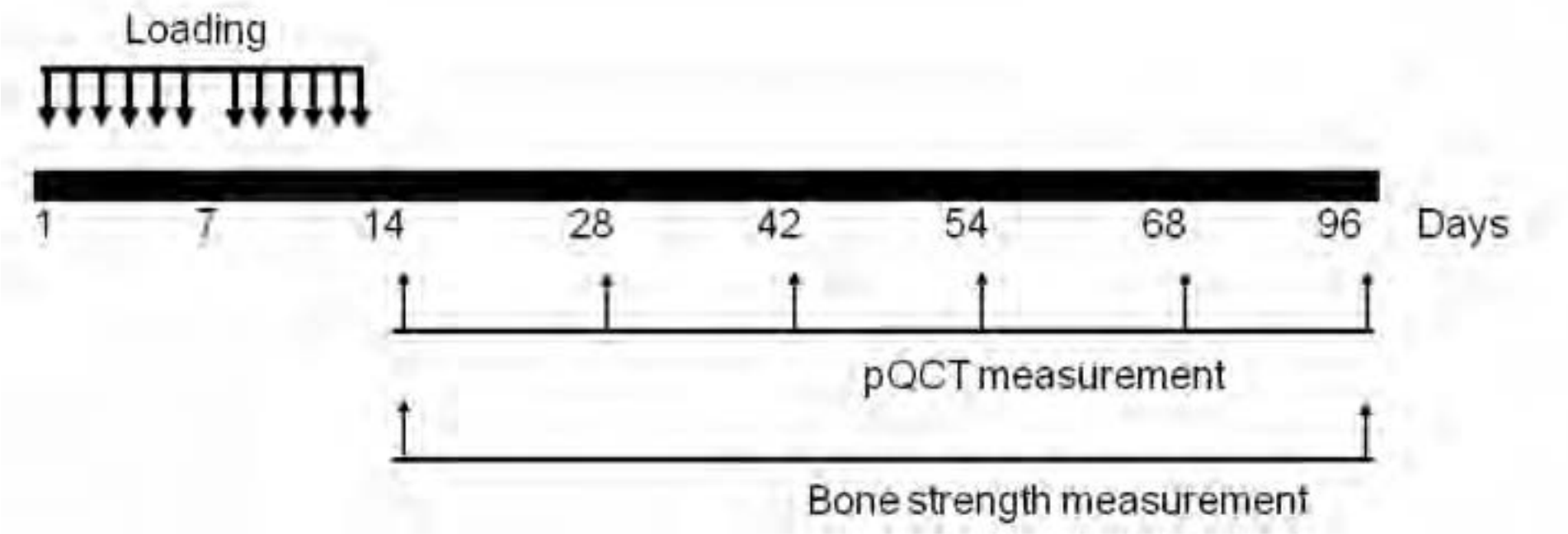

Fig2

Click here to download high resolution image

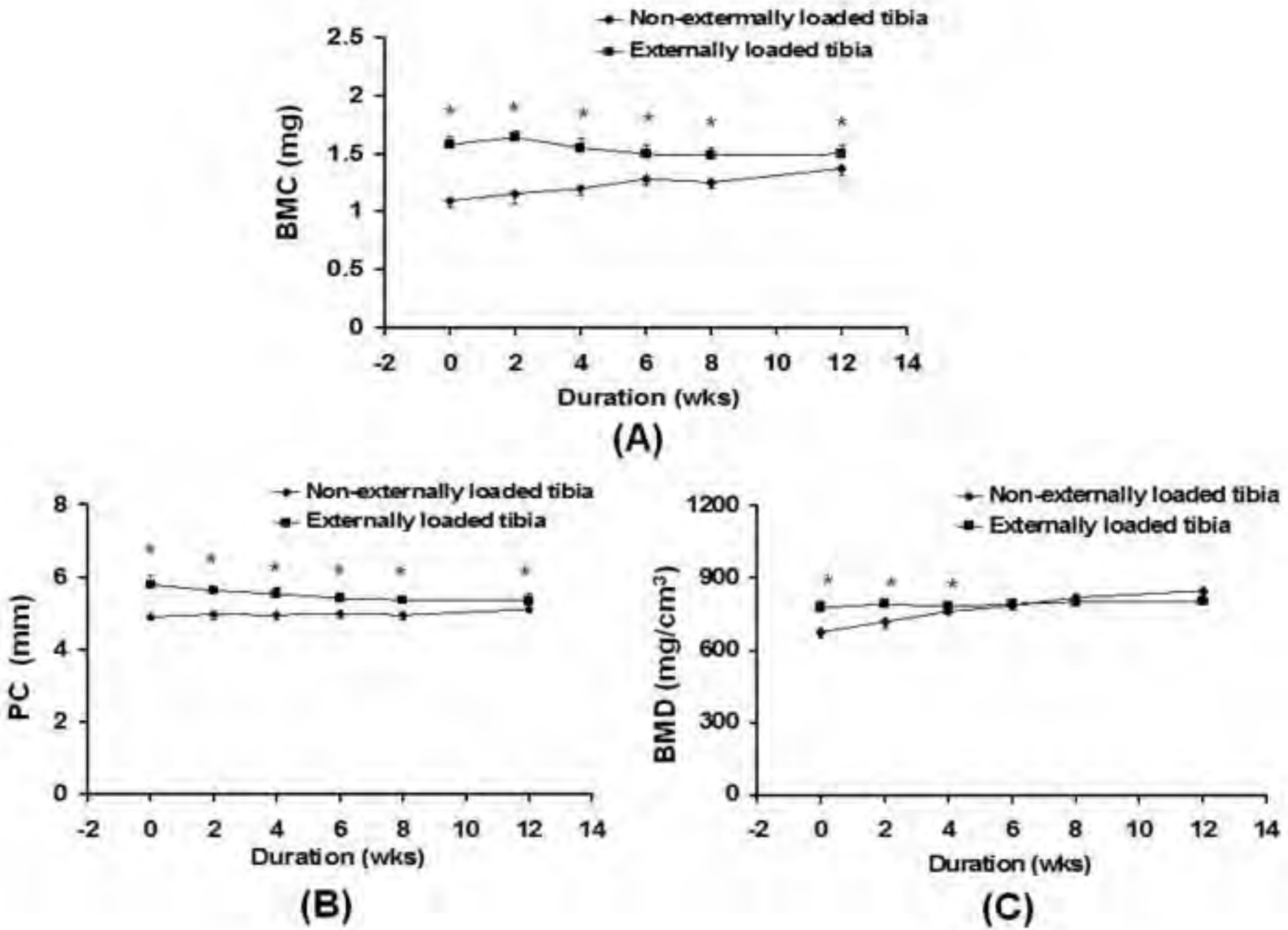

Fig3

Click here to download high resolution image

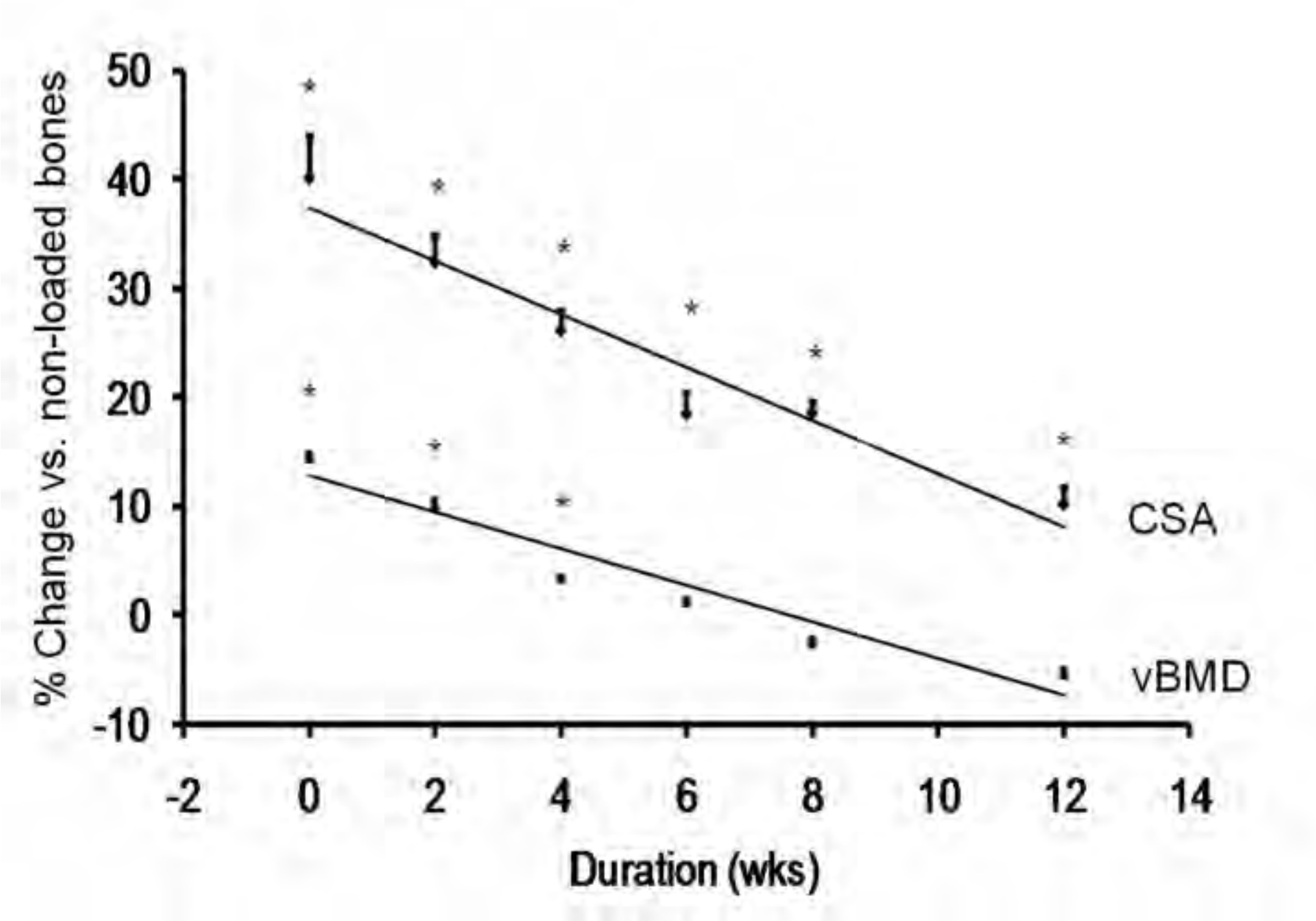

Fig4

Click here to download high resolution image

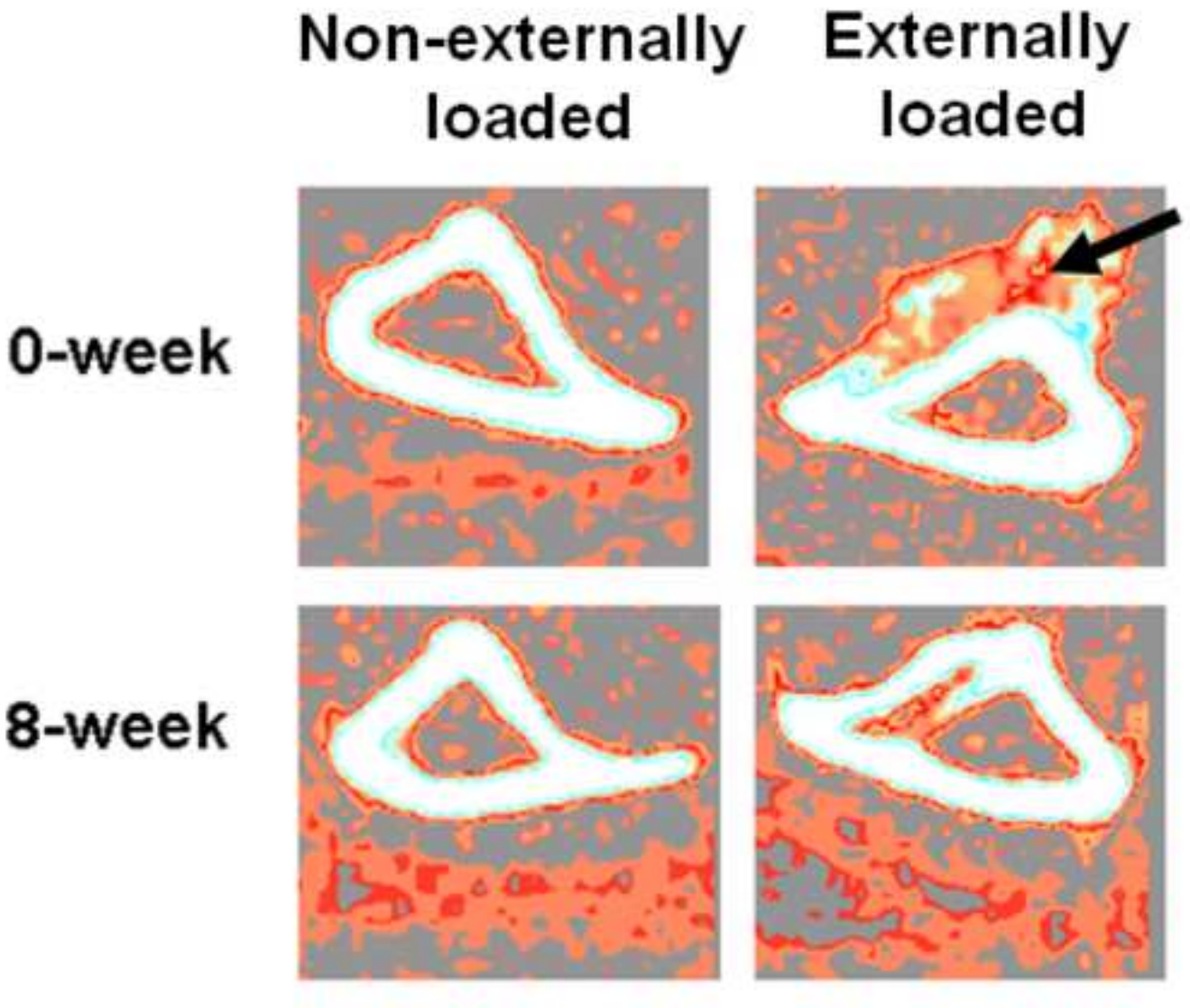

Table 1 Changes in mechanical properties of bone measured at 0- and 12-weeks after the cessation of last loading

Parameters	0 week		12 week	
	Non-externally loaded bone	Externally loaded tibia	Non-externally loaded bone	Externally loaded tibia
Yield load (N)	14.48 ± 0.42	20.34 ± 0.84*	17.08 ± 0.76	16.44 ± 0.71
Maximum load (N)	18.54 ± 0.67	24.05 ± 0.58*	21.93 ± 0.47	21.05 ± 0.17
Toughness (N/mm^2)	2.17 ± 0.05	3.10 ± 0.03*	2.03 ± 0.02	1.93 ± 0.14

Abbrevations: N, Newton
Values are mean ± SE with three-four mice per group
*$p<0.05$ vs. non-externally loaded bones